

## 4. SITE 567<sup>1</sup>

### Shipboard Scientific Party<sup>2</sup>

#### HOLE 567

Date occupied: 29 January 1982, 0345 hr.

Date departed: 30 January 1982, 2100 hr.

Time on Hole: 37 hr., 15 min.

Position: 12°42.96'N; 90°55.99'W

Water depth (sea level; corrected m, echo-sounding): 5500

Water depth (rig floor; corrected m, echo-sounding): 5510

Bottom felt (m, drill pipe): 5529

Penetration (m): 195.5

Number of cores: 2

Total length of cored section (m): 19.4

Total core recovered (m): 0.64

Core recovery (%): 3

##### Oldest sediment cored:

Depth sub-bottom (m): 195.5

Nature: mud

Age: early Pleistocene

Measured velocity (km/s): not measured

Basement: not reached

#### HOLE 567A

Date occupied: 30 January, 0345 hr.

Date departed: 7 February, 1032 hr.

Time on hole: 7 days, 9 hr.

Position: 12°42.99'N; 90°55.92'W

Water depth (sea level; corrected m, echo-sounding): 5500

Water depth (rig floor; corrected m, echo-sounding): 5510

Bottom felt (m, drill pipe): 5529

Penetration (m): 501.0

Number of cores: 29

Total length of cored section (m): 263.4

Total core recovered (m): 103.68

Core recovery (%): 39

##### Oldest sediment cored:

Depth sub-bottom (m): 368

Nature: limestone

Age: Late Cretaceous

Measured velocity (km/s): 2.884

##### Basement:

Depth sub-bottom (m): 368–501

Nature: ophiolite complex (basalt, diabase, gabbro, peridotites, serpentinites.)

Velocity range (km/s): 3.213 to 4.82

**Principal results (Holes 567 and 567A):** The sequence drilled at Site 567 confirms some conclusions from Leg 67, especially the results from Site 494: the base of the continental slope is not an accretionary prism of recent oceanic sediments but an extension of the terranes and framework geology underlying Central America.

Below the unconformity at the base of the Pliocene section that was recovered at Site 494, the sequence at Site 567 can be divided into three main sedimentary units and basement:

*Unit I.* 176 to 214.9 m: Pliocene–Pleistocene dark olive gray mudstone, which overlies Unit II in an unconformity also identified at Site 494.

*Unit II.* 214.9 to 318.2 m: early Miocene dark olive gray mudstone, with abundant angular to subrounded clasts of Late Cretaceous (Campanian), middle Eocene, and Oligocene lithologies, including a stratum of serpentinite pebbles (at 262.7 m) and some layers of blue gray mud probably derived from alteration of serpentinite.

*Subunit IIa.* 318.2 to 358.7 m: serpentinitic mud.

*Unit III.* 358.7 to about 368 m: Late Cretaceous (Campanian–Maestrichtian) pelagic limestone, highly fractured and with local veins.

**Basement:** about 368 to 501.0 m: a tectonically deformed ophiolite body, which can be divided into several subunits that are separated by sheared serpentinite, including:

*about 368 to 402.9 m:* a complex of gabbros and diabase that could be a dike complex;

*402.9 to 411.8 m:* sheared serpentinite;

*411.8 to 420.7 m:* gabbros and diabase;

*420.7 to 429.6 m:* sheared serpentinite;

*429.6 to 501.0 m:* from top to bottom, basalts with some indication of pillow lavas (429.6–438.5), diabase and gabbros (438.5–465.2), and peridotites (harzburgites, 465.2–501.0); this succession is a characteristic ophiolite but of greatly reduced thickness because of numerous faults;

*501.0 m:* a piece of basalt recovered in the last core catcher indicates that perhaps another subunit underlies the preceding ones. The depth at which the drill hole became unstable may have been very close to the top of the zone that is intensely deformed by subduction.

The serpentinite of Subunit IIa is probably a large displaced body at the base of the early Miocene mudstone transported in a similar way as the serpentinite and other lithic fragments that are clasts in the mudstone because the serpentinite unit is underlain by thin (stratified?) Miocene mudstone. The Late Cretaceous Unit III appears to be (1) a block displaced from upslope, despite the absence of early Miocene below this unit; (2) the normal sedimentary cover of the ophiolite of Unit IV; or (3) sedimentary rocks involved in the tectonic emplacement of the ophiolites.

Although there are some differences in the depths of various biostratigraphic units, the results from Site 494 only 110 m away can be interpreted consistently with the large early Miocene unit

<sup>1</sup> von Huene, R., Aubouin, J., et al., *Init. Repts. DSDP*, 84: Washington (U.S. Govt. Printing Office).

<sup>2</sup> Roland von Huene (Co-Chief Scientist), U.S. Geological Survey, Menlo Park, California; Jean Aubouin (Co-Chief Scientist), Département de Géotectonique, Université Pierre et Marie Curie, Paris, France; Miriam Baltuck, Scripps Institution of Oceanography, University of California, San Diego, La Jolla, California (present address: Department of Geological Sciences, Tulane University, New Orleans, Louisiana); Robert Arnott, Department of Geology, University of Oxford, Oxford, United Kingdom (present address: Shell International, The Haag, Holland); Jacques Bourgois, Département de Géotectonique, Université Pierre et Marie Curie, Paris, France; Mark Filewicz, Union Oil Company, Ventura, California; Roger Helm, Institut für Geologie, Ruhr-Universität Bochum, Bochum, Federal Republic of Germany; Keith A. Kvenvolden, U.S. Geological Survey, Menlo Park, California; Barry Leinert, Hawaii Institute of Geophysics, University of Hawaii, Manoa, Honolulu, Hawaii; Thomas J. McDonald, Department of Oceanography, Texas A&M University, College Station, Texas; Kristin McDougall, U.S. Geological Survey, Menlo Park, California; Yujiro Ogawa, Department of Geology, Kyushu University, Hakozaki, Fukuoka-Shi, Japan; Elliott Taylor, Department of Oceanography, Texas A&M University, College Station, Texas; Barbara Winsborough, Espey, Houston, and Associates, Austin, Texas (present address: Department of Geology, Princeton University, Princeton, New Jersey).

containing a sedimentary breccia of serpentinite at Site 567, but these results still leave open the interpretation of the Late Cretaceous. On land, Campanian-Maestrichtian pelagic limestones were deposited unconformably on the ophiolitic complex of the Santa Elena Peninsula of Costa Rica, whereas in northeast Guatemala ophiolites overthrust Maestrichtian limestones. Either could be a parallel to the relation between the limestone and ophiolitic rocks at Site 567.

The limestone and ophiolitic rock of Site 567 are considerably older than the rocks of the Cocos Plate. On the Cocos Plate the chalks overlying the igneous ocean crust are Miocene.

The main new finding of Site 567 is that the lower slope of the Trench is an ophiolitic complex that underwent intense tectonic deformation not related to the present subduction zone, and was assembled in its present form prior to the early Miocene, because the complex was eroded and incorporated into the overlying early Miocene slope deposits as pebbles and probably also as big blocks. During the early Miocene this ophiolitic complex cropped out upslope and was sufficiently unstable to shed large quantities of debris downslope. The complex, older than the middle Eocene, may be compared with the ophiolite complexes of Central America. There is no accretionary prism of recent oceanic material in front of the ophiolitic complex at the base of the slope.

### BACKGROUND AND OBJECTIVES

Site 567 is about 3 km upslope from the floor of the Middle America Trench and about 550 m higher, situated on the first in a series of benches that mark this area of the landward slope of the Trench.

This same site was partially drilled on Leg 67, and despite only partial completion it was the only Leg 67 site to penetrate the slope deposits and sample the pre-Neogene sequence beneath. The major objective of this leg was to sample below the slope deposits across a transect of sites. It had been predicted from geophysical data that below the slope deposits at Site 494 there would be an imbricated sequence of Pleistocene trench deposits, but instead an Upper Cretaceous to lower Miocene section was found. Part of Leg 67 was spent unsuccessfully trying to complete the drilling at Site 494, which had been stopped for a downhole experiment and not because of drilling difficulty. Site 567 provided the opportunity to complete the drilling begun at Site 494.

Because of the difficulty in relating the section cored at Site 494 to the tectonic history of the Guatemalan convergent margin, more geophysical work was done after Leg 67. As a result of the geophysics, some of the original ideas about the site were modified. Reprocessing of the major seismic reflection data revealed more clearly the depth of slope deposits and the lack of any deformation in trench sediment entering the subduction zone (von Huene et al., 1982).

A Seabeam survey (Aubouin et al., 1981) revealed a remarkable subduction of ocean ridges without significant topographic disturbance of the trench-slope junction. A deep-tow survey indicated little deformation near the seafloor, especially for the front of a subduction zone. Site 494 appears to be removed from any near-surface tectonic structure (Moore et al., 1982). The results of refraction measurements during deployment of the downhole seismometer verify previous less sophisticated seismic velocity measurements along the transect (Ambos and Hussong, this volume). The geophysical studies in progress certainly indicate less than chaotic deformation at the front of the margin despite subduction of 500-m

ridges on the ocean floor. The seismic records contain faint reflections that appear to be from the subducted sediment, as Site 494 data indicated.

The objectives at Site 567 were to penetrate the unsampled section below the Cretaceous marls at the bottom of 494 and perhaps enter the subduction zone. The physical condition of rock in a subduction zone is a key to understanding why the subduction of 100 km of ocean crust each million years can be accommodated with so little disruption of the front of the margin.

### OPERATIONS

*Glomar Challenger* departed from Hole 566C at 2215L (local time), 28 January, and approached Site 567 at midnight. At 0034L, 29 January, a 16 kHz beacon was dropped at the best approximation of position and bathymetry for Site 567. Making up the drill string took from 0345 to 1030L the same day, during which time sufficient satellite positions were received to establish a precise beacon position. Between 1030 and 1730L *Glomar Challenger* made an offset of 2867 ft. from the beacon on bearing 226° in order to occupy the position of Hole 494A. Hole 567 was spudded at 1840L and drilling operations began, washing out the first 176 m, which had been identified as Pleistocene at Site 494.

The wash core was recovered at 2345L, 29 January and the first core came up at 0230L 30 January. The second was cut from 0230 to 0445L but it was impossible to retrieve the core barrel, which became stuck in the bit. After four unsuccessful attempts at retrieving the core barrel it was necessary to retrieve the drill string, which we accomplished at 2100L 30 January. The core barrel was found jammed metal to metal into the upper part of the core guide; the core barrel contained only cavings and cuttings.

Assembly and lowering of the drill string for Hole 567A began at 2345L, 30 January. At 1015L, 31 January, the hole was spudded and drilling began, washing out to 195.5 m. The first core was recovered at 1718L, 31 January, and contained, as expected, Pleistocene mudstone.

On 2 February, 0950L, Core 15 came up empty because of a plugged bit. From 1000 to 1315L the bit was unplugged and drilling resumed. Three more cores were recovered in serpentinite prior to 3 February, 0045L. The drilling times increased at Core 13, and recovery became very poor in the first serpentinite. Cores 19 and 20 were retrieved after drilling two joints. Normal coring resumed when harder rock, presumably different from the serpentinites was entered; Core 21, recovered on 3 February, 1550L, contained gabbros and basalts.

The drilling times increased to more than 20 min./m and the lithology remained identical, so on 4 February permission was requested from DSDP to recover the core barrel after drilling two joints, in order to meet objectives in the time available for this site. Permission was given under two conditions: that there was no indication of substantial accumulation of migrated hydrocarbons; and that normal core barrel retrieval procedure would resume when drilling beyond the top of the subduction zone. On 5 February, Cores 27, 28, and 29 were cut and recovered in this way.

After the recovery of Core 28, at 1015L, 5 February, the drill pipe became stuck. At 1115L, after we worked on this sticking pipe, Core 29 was cut with great difficulty; the pipe stuck as mud came through the bit, and after again working the stuck pipe from 1815 to 2030L, Core 29 was retrieved at 2200L. Bit release operations were from 2200 to 2400L, 5 February, while we were encountering possible overpressure formation (overpressure 520 lb.) that could have indicated one of the contacts related to the subduction zone.

After hole preparation, the logging began at 0800L, 6 February; induction, sonic, gamma-ray, and caliper logs were run. The hole bridged at 5800 m, and two logging runs were made in the upper part of the hole. The drill pipe was then lowered past the bridge and to within 100 m of total depth before it stopped. The hole was again conditioned with mud, and logging was attempted with the end of the pipe hanging just beyond the depth of the bridge. However, the pipe had become jammed with material despite continuous circulation, and it could not be cleared sufficiently for logging by dropping the logging tools. During retrieval of the tools, at 1100L, 7 February, the drill pipe failed a short distance beneath the ship and, with a great shudder that was felt throughout the ship, about 5000 m of pipe, logging tools, and a bottom-hole assembly parted and fell to the seafloor. A new joint of drill pipe, put into the string for the first time, had fatigued despite calm seas, no rotation, and without the string becoming stuck during the logging operation. Everyone was grateful that no injuries occurred as the broken end of the logging cable came whipping across the rig floor, and we quickly counted the remaining joints of drill pipe to see if the shallower sites could still be drilled.

Table 1 shows the coring summary.

## LITHOSTRATIGRAPHY AND IGNEOUS PETROLOGY

### Lithostratigraphy

Site 567 is located at the base of the lower slope of the Middle America Trench, about 5 km north of the Trench axis (Fig. 1). Two holes were drilled, 567 and 567A. Hole 567 was drilled where the seafloor is 5529 m below sea level. One core (H1) was taken after washing down to 5705 m, and two cores were recovered before the hole was abandoned because of technical difficulties. Hole 567A was also drilled where the seafloor is 5529 m below sea level. The core barrel was recovered after washing down to 5724 m, and the remainder of the hole was cored continuously down to 501 m sub-bottom. The samples recovered from both holes provide a good record of the stratigraphy.

The sediments can be divided into three units on the basis of their lithology (Fig. 2).

### Unit I

Unit I comprises Cores H1, 1, and 2 in Hole 567; and in Hole 567A, Cores H1, and 1 to 3; 176 to 214.9 m sub-bottom depth (Pliocene to Pleistocene).

**Major lithology:** This unit is composed of a dark olive gray (5Y 4/2) siliceous mud and a grayish olive green

mud (5GY 3/2) that unconformably overlies Unit II. This unconformity was observed at Site 494.

Sedimentary structures are rare, but some thin laminations were observed in Hole 567A, Core 3. Small sub-rounded to subangular pebbles of bluish gray (5BY 4/1) mud as well as dispersed sand grains are common in Hole 567A, Cores 1 and 2. Light olive gray (5Y 5/2) and light gray (5Y 7/1) mottling of the mud in Core 567A-2 is the result of bioturbation.

The average sand-silt-clay percentages for this unit are 8, 19, and 73%, respectively (based on shipboard smear-slide analyses). The major detrital component is clay, although minor amounts of quartz, plagioclase feldspar, and other terrigenous materials are present. Glauconite and pyrite occur in quantities less than 4%.

Well-preserved diatoms and sponge spicules account for up to 19% of the composition of the mud. Foraminifers are rare and of mediocre preservation. Some unspecified carbonate detritus (in concentrations of up to 12% of the total sediment) may occur in broken foraminifer tests. Large shell fragments were observed in Hole 567, Core H1.

**Minor lithology.** This unit also comprises a dark grayish olive (5Y 3/2) sand only observed in Core 567A-2. The sand is present in graded beds up to 5 cm thick. Erosional bases were noted. Internal sedimentary structures are rare, but some parallel alignment of grains was observed. The major detrital components are clay and quartz, although minor amounts of plagioclase feldspar and rock fragments are present.

### Unit II

Unit II comprises Cores 567A-3 to -18; 214.9 to 358.7 m sub-bottom depth (early Miocene). This unit is differentiated from the overlying sediment by its age and by the presence of sedimentary breccias and large transported boulders in the lower part. The contact with Unit I is not clearly defined in Core 3, but paleontology suggests that it lies between Sections 1 and 3 of this core (see Biostratigraphy).

**Major Lithology.** This unit is made up of a grayish olive green (5GY 3/2) to dusky yellowish green (10GY 3/2) early Miocene mud. This mud encloses clasts of varying lithologies and ages (see discussion that follows). Sedimentary structures within the mud are rare, but some thin laminations were observed in Cores 6 and 18. Mottling of the mud is present throughout this unit, caused by bioturbation. Postdepositional fracturing of the mudstone is common, particularly near the top of the unit. Sand-silt-clay percentages for the mud are 5, 15, and 80%, respectively (based on shipboard smear-slide analyses). The major detrital component is clay, although minor amounts of quartz and plagioclase feldspar are present.

The dominant feature of this unit is the presence of sedimentary breccias. The average clast size is about 1 cm in diameter but ranges from about 3 mm to 50 cm in diameter. The breccias are commonly clast supported, but some matrix-supported sections are observed. There is no parallel alignment or internal sorting of clasts. Individual beds could not be identified because of the generally "massive" nature of the breccias.



Table 1. Coring Summary, Site 567.

Core	Date (Jan.-Feb. 1982)	Time	Depth from drill floor (m)		Depth below seafloor (m)		Length cored (m)	Length recovered (m)	Recovery (%)
			Top	Bottom	Top	Bottom			
Hole 567									
H1	29	2345	5529.0	5705.1	0.0	176.1	—	—	—
1	30	0025	5705.1	5714.8	176.1	185.8	9.7	0.10	1
2	30	2130	5714.8	2724.5	185.8	195.5	9.7	0.54	6
Total							19.4	0.64	3
Hole 567A									
H1	31	1718	5529.0	5724.5	0.0	195.5	—	—	—
1	31	1913	5724.5	5734.2	195.5	205.2	9.7	6.10	65
2	31	2344	5734.2	5743.9	205.2	214.9	9.7	9.45	97
3	Feb. 1	0227	5743.9	5753.6	214.9	224.6	9.7	9.72	94
4	1	0430	5753.6	5763.1	224.6	234.1	9.5	4.38	46
5	1	0630	5763.1	5772.6	234.1	243.6	9.5	6.90	73
6	1	0832	5772.6	5782.1	243.6	253.1	9.5	6.62	70
7	1	1203	5782.1	5791.7	253.1	262.7	9.6	3.03	32
8	1	1433	5791.7	5800.9	262.7	271.9	9.2	6.76	73
9	1	1705	5800.9	5809.7	271.9	280.7	8.8	6.87	78
10	1	1906	5809.7	5818.5	280.7	289.5	8.8	9.10	100
11	1	2133	5818.5	5827.4	289.5	298.4	8.9	2.39	27
12	2	0038	5827.4	5836.3	298.4	307.3	8.9	7.13	80
13	2	0345	5836.3	5845.2	307.3	316.2	8.9	2.52	28
14	2	0653	5845.2	5854.1	316.2	325.1	8.9	2.88	32
15	2	0950	5854.1	5863.0	325.1	334.0	8.9	0.00	0
16	2	1630	5863.0	5871.8	334.0	342.8	8.8	2.35	27
17	2	1930	5871.8	5880.7	342.8	351.7	8.9	3.73	42
18	3	0045	5880.7	5887.7	351.7	358.7	7.0	1.20	17
19	3	0540	5887.7	5897.4	358.7	368.4	9.7	1.35	14
3 Drilled		5897.4–5905.4	368.4	376.4	—	—	—	—	—
20	3	1039	5905.4	5915.1	376.4	386.1	9.7	1.22	13
3 Drilled		5915.1–5923.1	386.1	394.1	—	—	—	—	—
21	3	1550	5923.1	5931.9	394.1	402.9	8.8	0.30	3
22	3	2127	5931.9	5940.8	402.9	411.8	8.9	0.22	2
23	4	0125	5940.8	5949.7	411.8	420.7	8.9	0.50	6
24	4	0645	5949.7	5958.6	420.7	429.6	8.9	1.60	18
25	4	1205	5958.6	5967.5	429.6	438.5	8.9	2.70	30
26	4	1834	5967.5	5974.8	438.5	445.8	7.3	0.60	8
27	5	0050	5974.8	5984.5	445.8	455.5	9.7	1.00	10
5 Drilled		5984.5–5994.2	455.5	465.2	—	—	—	—	—
28	5	1015	5994.2	6003.9	465.2	474.9	9.7	1.10	11
5 Drilled		6003.9–6013.6	474.9	484.6	—	—	—	—	—
29	5	2210	6013.6	6023.3	484.6	494.3	9.7	1.96	20
5 Drilled		6023.3–6030.0	494.3	501.0	—	—	—	—	—
Total							263.4	103.68	39

Note: H1 designates wash core. "Drilled" in Time column indicates that recovery was combined with recovery of the preceding core, that is, two core lengths were drilled for every instance of recovery.

The lithologies of clasts observed within the breccia are listed as follows:

1. Eocene to Miocene mudstone clasts (Cores 3–6). Color: Pale green (10GY6/3), bluish gray (5B 5/1).
2. Pumice clasts (Core 8).
3. Light gray limestone Eocene clasts (Cores 12, 13, 18).
4. Light greenish gray Cretaceous (late Campanian) nannofossil ooze clasts (Cores 12, 13, and 18).
5. Sandstone clasts (Core 13).
6. Medium gray mud mixed with bluish gray limestone of the Cretaceous (Cores 12, 13).
7. Serpentinite (Cores 7 and 14 to 18).

**Minor Lithologies.** The first minor lithology comprises a grayish green (5G 5/2) conglomerate that contains rounded clasts up to 5 cm in diameter (Core 10). The conglomerate is clast-supported and has a sparse mudstone matrix. No internal sorting of clasts was observed. Clasts within the conglomerate include limestone, andesite, and green mud.

The second minor lithology comprises a dusky blue (5P B3/2) to grayish blue (5PB 5/2) mud (Core 7). It is composed of serpentine (80%) and dolomite (15%).

The third minor lithology comprises volcanic ash (Cores 6 and 8) with up to 50% quartz grains. Only two ash layers were observed; but both are graded, suggest-



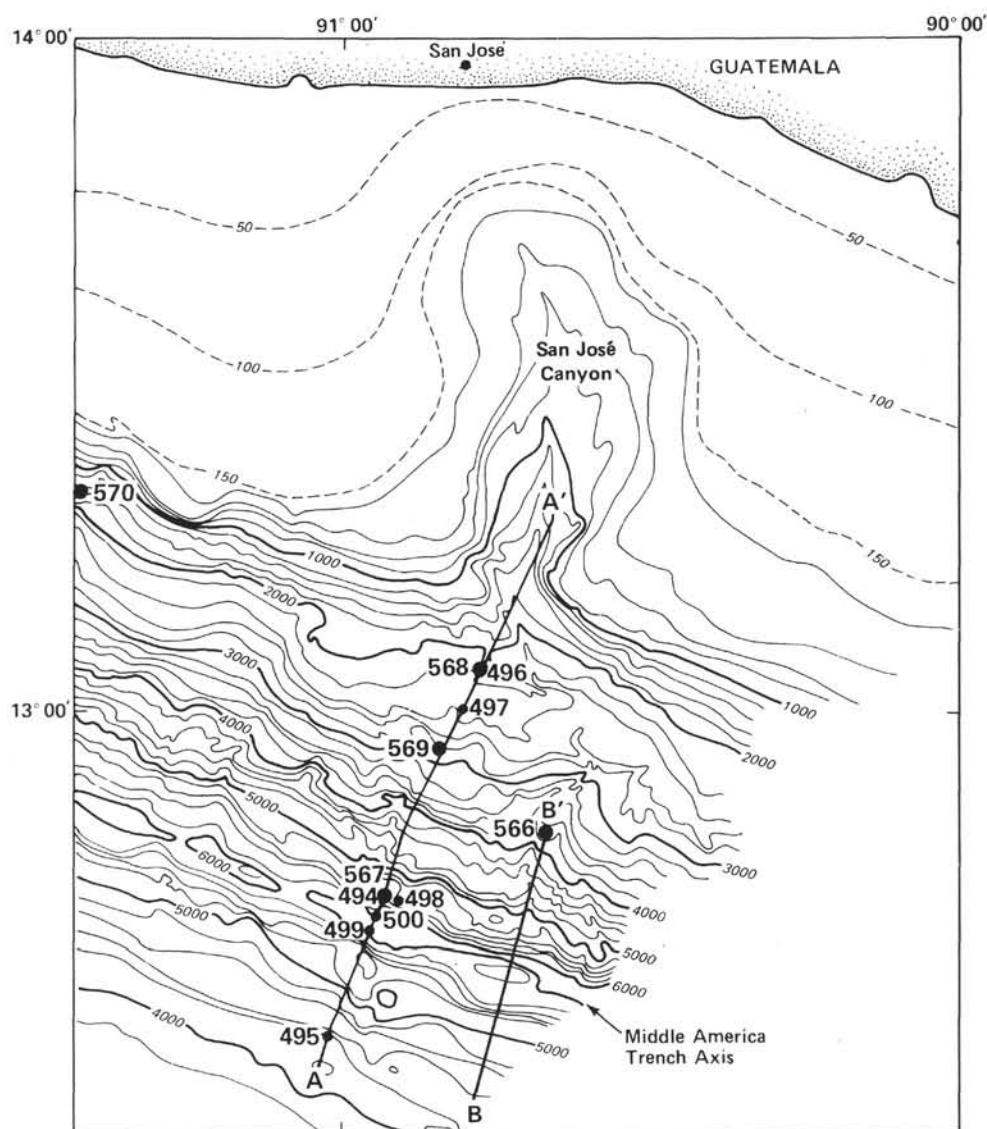


Figure 1. Bathymetry of the Guatemala margin and San José Canyon, showing the UTMSI survey track and the location of Legs 67 and 84 sites off Guatemala.

ing deposition by a turbidity current rather than by air fall.

#### **Subunit IIa**

Subunit IIa, Cores 14 to 18, 318.2 to 358.7 m sub-bottom, comprises a thick sequence of serpentinitic mud with serpentinite clasts, pale blue green (SBG 7/2) and grayish blue (SPB 5/2) (Cores 14 to 18). It is separated from the underlying Unit III by early Miocene mud. It has been included as a subunit of Unit II because it is underlain and overlain by the Miocene mud of Unit II. The massive serpentinitic mud can be interpreted as a debris flow that has incorporated sediment of unknown age. The nature of the contact between the serpentinitic mud and Miocene mud that underlies it(?) in the core is unclear (see Frontispiece to volume).

#### **Unit III**

Unit III comprises Core 567A-19, 358.7 to about 368 m sub-bottom (Late Cretaceous).

**Major lithology:** This unit is composed of a pale red (10R6/2) to pale greenish yellow (10Y 8/2) Late Cretaceous limestone. No sedimentary features were observed because of the recrystallization and deformation structures present. These include calcite veins and small fractures.

The upper and lower contacts of this unit were not recovered, so it is difficult to know the relationship of Unit III with the underlying basement and overlying early Miocene Unit II.

#### **Basement**

Basement (Cores 20 to 29; about 368 m to 501 m sub-bottom) is composed of an unordered sequence of gabbro, diabase, basalt and serpentine and has been variably metamorphosed and complexly deformed. Figure 3 provides a general description of the nature of the basement.

Within the 135 m of basement drilled, recovery was poor, but four main types of igneous rock were recovered.

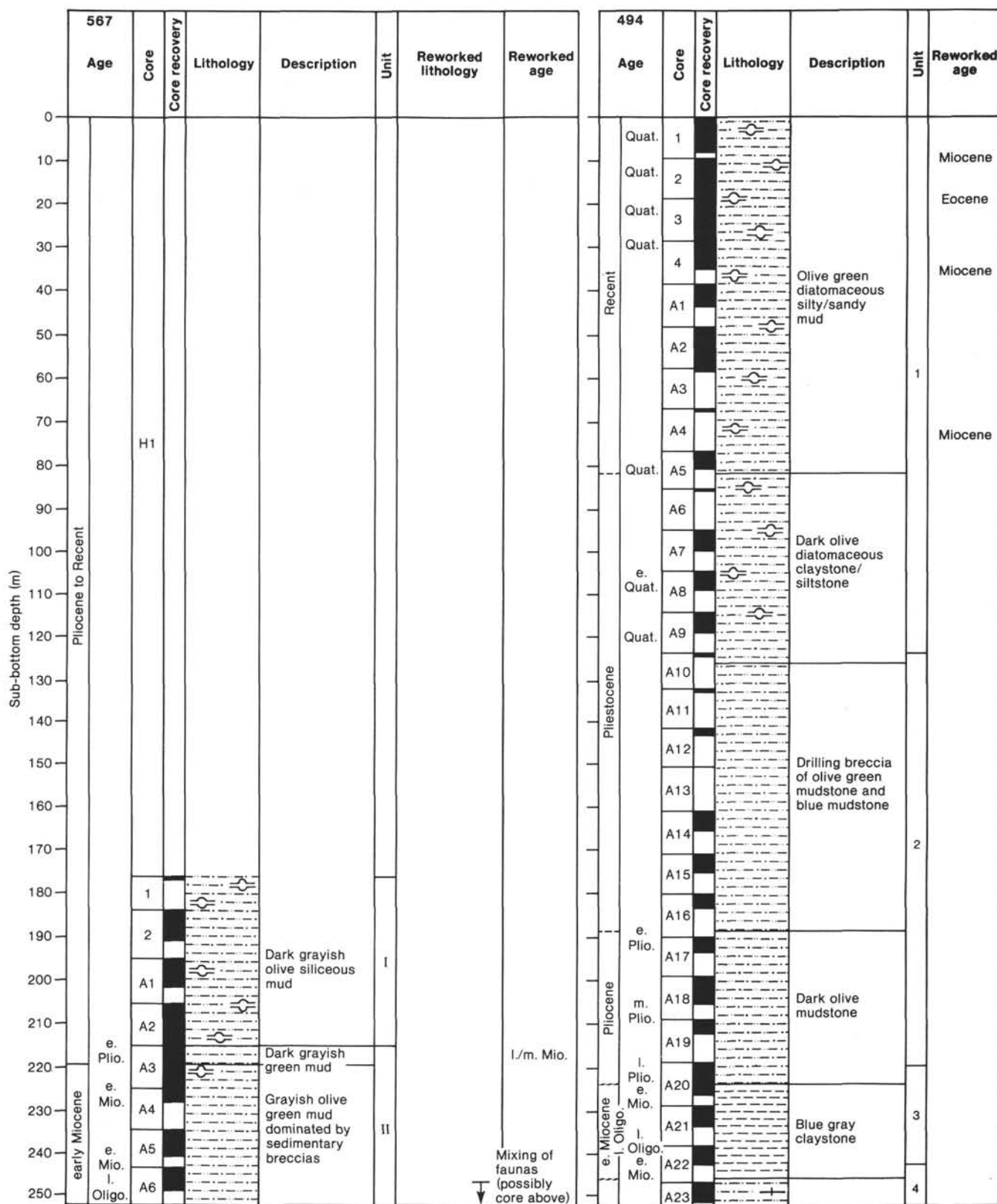


Figure 2. Lithostratigraphic summary of Sites 567 and 494. (The extra length of Cores 567A-19, 20, 27-29 is explained in Table 1.)

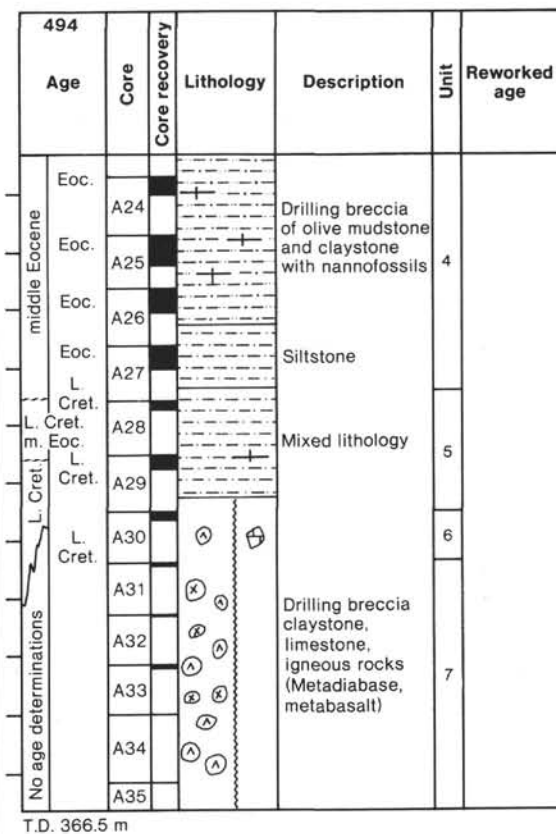
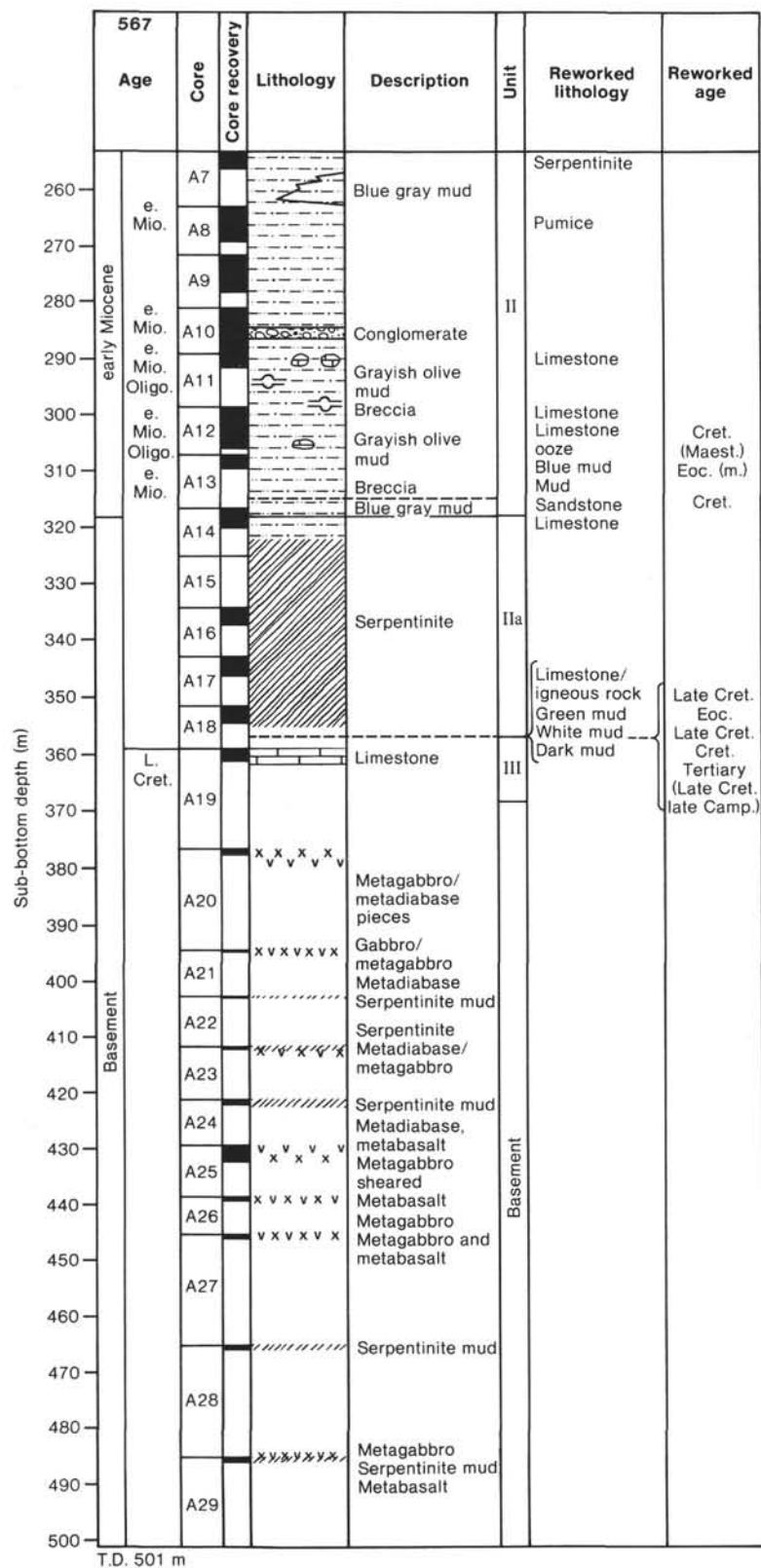


Figure 2. (Continued).



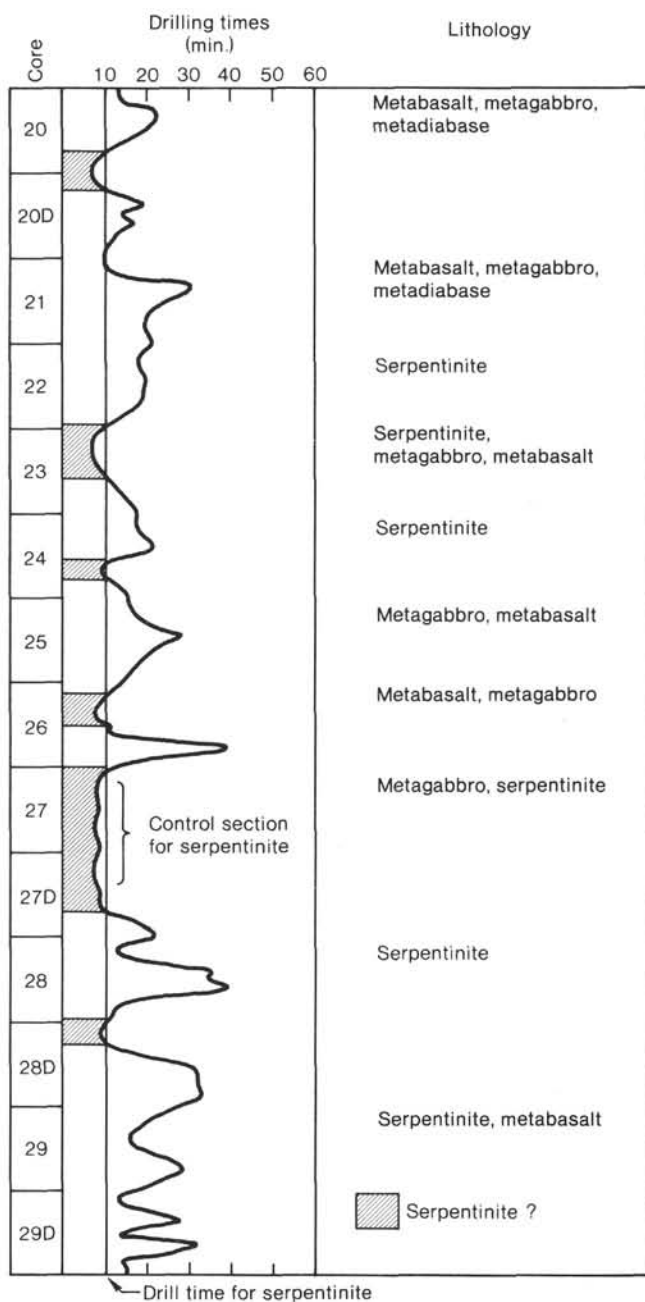


Figure 3. Drilling time correlated with basement rock types at Hole 567A. (Cores with a D suffix indicate that two core lengths were drilled for every instance of recovery.)

ered. No apparent sequences were recovered (e.g., from gabbro to diabase to basalt). Three main zones of altered serpentinite were recovered (Cores 22–23, 27, and 29), and these may coincide with three main fault zones. Small amounts of altered serpentine were observed within sections of Cores 23 and 25, perhaps representing smaller dislocations. The petrology and deformation of basement rocks is discussed in the Igneous Petrology section that follows.

## Igneous Petrology

At Site 567 several types of igneous rock were recovered, including ultramafic rocks, gabbros, diabases, and basalts. The petrology of these rocks is described next.

### Ultramafic Rocks

#### *Serpentinite with Mesh and Ribbon Textures* (567A-14-2, 134–137 cm; 567A-7-2, 40–41 cm)

The only vestiges of primary minerals in the serpentinite are chromite (1%) and orthopyroxene (which is indicated as a serpentine pseudomorph). The serpentine exhibits mesh and ribbon textures. Opaque minerals are quite common but are often elongated parallel to the serpentine minerals. Some kinking of the orthopyroxenes preserved within bastite crystals is also seen. Chrysotile veins crosscut all the minerals just described.

#### *Serpentinite—Platy Bastite Type* (567A-14-2, 142–144 cm)

The only remnant primary mineral present in this sample is brown red chromite (2%), which exhibits a porphyroblastic texture. About 90% of the rock is composed of clay, pavement-texture serpentine. Individual serpentine crystals (lizardite, bastite) have an average length of 1.5 mm. Serpentine pseudomorphs are seen to preserve shear bands within original orthopyroxenes. The high bastite content of the rock (about 90%) suggests that the original mineralogy was dominated by orthopyroxenes. Younger shear zones crosscut the rock and are filled with serpentine (chrysotile).

### Gabbros

Gabbroic rocks recovered at Site 567 include layered metagabbros, massive metagabbros, and ophitic micro-metagabbros.

#### *Metagabbro with Hypidiomorphic Textures* (567A-20-1 [Piece 1]; 567A-20-1 [Piece 9]; 567A-20-1 [Piece 2]; 567A-21, CC [13–15 cm])

These samples of metagabbro exhibit a hypidiomorphic to granular texture. Labradorite to bytownite feldspar is the primary mineral, and laths range in length from 1 to 5 mm. The feldspars have been moderately altered to clay minerals, hydrogarnet, and chlorite. Green to brown diopside and augite clinopyroxenes are also abundant and range in size from 0.55 mm to 2 mm in diameter. The clinopyroxenes are strongly altered to actinolite and chlorite. Opaque minerals are absent.

This rock exhibits a postalteration tectonism. Shear bands and kinking of actinolite are common. Crosscutting veins are first filled by zeolites and then by quartz.

#### *Micrometagabbro with Ophitic Texture* (567A-26-1 [Piece 15]; 567A-25-1 [Piece 7])

These samples have an ophitic framework of plagioclase laths, up to 2 mm in length, that is filled by green to brown clinopyroxenes. Plagioclase appears to be more

altered than the clinopyroxene. The main alteration products are chlorite and actinolite. Euhedral magnetite is also quite abundant. Kinking of actinolite crystals is present as well as late-stage zeolite and calcite veins.

### Diabases

#### *Weakly Altered Diabase (567A-19, CC)*

This rock has an ophitic to subophitic texture with a framework of labradorite laths up to 0.5 mm in length. Diopside to augite clinopyroxenes are concentrated around the feldspars. Chlorite and actinolite are abundant alteration products. Zeolites and quartz are present within crosscutting veins.

#### *Strongly Altered Diabase (567A-20-1 (Piece 8))*

This rock displays a microlitic texture of actinolite that has replaced the clinopyroxenes. The groundmass has been replaced by chlorite and prehnite with secondary magnetite dispersed throughout the rock. No deformation structures are observed, but zeolites and quartz are present in veins that crosscut the diabase.

### Basalts

Abundant palagonite (common alteration product of volcanic glass) is present in this rock, indicating formation within a subaqueous environment. The main texture of the rock comprises plagioclase laths dispersed within a glassy altered groundmass.

### Comments

From the description of the thin sections, this summary of metamorphic and deformation events for the Site 567 basement rocks can be inferred: (1) formation of the igneous rock (different for each rock type); (2) metamorphic grades (different for each rock type); (3) deformation—predominantly shearing (common to all samples examined); (4) calcite and zeolite veins (common to all samples examined).

The timing of these events is unknown but the rock types recovered may have been derived from an ophiolite complex, and it is likely that the first two events occurred at a higher temperature. Each of the samples examined displays a different metamorphic history, from zeolite facies in the basalts and diabases to greenschist facies in the gabbros. Similar differences and grades of metamorphism are observed in present-day oceanic crustal rocks and also within ophiolite complexes.

### Diagenesis and Clay Mineralogy

Authigenic pyrite is a common diagenetic feature within the muds of Site 567. Pyrite in Cores 567A-1 to -17 shows no crystal forms and may actually be amorphous FeS<sub>2</sub>. In Cores 567A-18 to -23 the characteristic cubic form of pyrite was observed.

The dominant lithology from Cores 567A-1 to -6 is grayish green mud; XRD (X-ray diffraction) analysis of this mud shows a badly defined "peak" encompassing

clay mineral d-spacings between 25 and 12 Å. This clay mineral assemblage is related to the alteration of volcanic material, even though unaltered plagioclase, hornblende, and glass are present. Silica occurs as both opal-a and opal-ct in adjacent biogenic siliceous skeletons, which implies a mixing of fossil material, also documented by paleontological data (see Biostratigraphy).

Clasts and beds of a grayish blue mud occurred in Cores 567A-2, 3, and 5. XRD data of this mud show a distinct 14 Å d-spacing of a smectitelike clay mineral together with a very weak 7 Å d-spacing, probably due to a chlorite. The formation of this blue mud may be related to the weathering of volcanic material, because there was a large amount of volcanic fragments present.

Bright blue serpentine mud occurs in Core 7, interbedded with green mud. This blue mud is only composed of serpentine and a carbonate mineral from the hydrotalcite group (based on shipboard X-ray). A remarkable amount of smectitic clay minerals occurs in the green mud interbedding the blue mud; most probably these minerals were derived from altered volcanic material.

A white mud in Core 23 that is composed of talc and serpentine is probably an alteration product of serpentine. In Cores 567A-17, 18, and 24, white mud beds contain 14 Å to 15 Å smectites (shifting to 17 Å after treatment with glycol) and 12 Å Na-montmorillonite (shifting to 17 Å after treatment with glycol). Large amounts of volcanic glass, zeolites, or apatite in smear slides from these beds indicate that they contain strongly altered tuffaceous material.

### Summary

The source of the early Miocene mud in Units I and II is probably the reworked and weathered Tertiary volcanic outcrops of Guatemala. Benthic foraminifers demonstrate that much of the Miocene sediment of Unit II was transported from the depth of the site of the Esso Petrel Well (see Biostratigraphy). During the early Miocene there was considerable erosion on the shelf, probably related to a relative lowering of sea level. Many of the Miocene mud clasts recovered at Site 567 may have been transported from this area. Reworked Eocene, Cretaceous, and serpentinite clasts may have been derived from exposures on the steep parts of the upper to mid-slope areas (of the landward side of the Middle America Trench) where suitable rocks may crop out. The Late Cretaceous limestone (Unit III) is representative of an open ocean environment, the absence of detrital grains indicating that deposition occurred far from the influence of hemipelagic sedimentation.

The basement rock recovered at Site 567 is composed of an unordered sequence of gabbro, diabase, basalt, and serpentinite that has been variably deformed and metamorphosed. The repeated juxtaposition of these four rock types indicates that the basement has been highly tectonized. Deformation occurred before the deposition of the slope deposits, that is, pre-Miocene or possibly pre-Late Cretaceous. It is clear that the deformation of the basement is not related to the present-day tectonic

setting of subduction (that commenced in the Oligocene) but is related to an earlier and different tectonic setting.

## BIOSTRATIGRAPHY

### Introduction

Two holes at Site 567 recovered early Pleistocene, Pliocene, and early Miocene mudstones above a mixed sequence of Oligocene, middle Eocene, and Late Cretaceous angular lithic fragments associated with an early Miocene mud matrix (567A-11 through 567A-13, CC; Fig. 4). Cores 567A-14 through 18 recovered blue serpentinite mud and are barren of all microfossils. In 567A-18, CC the possible lower contact of the blue mud rests on a gray mudstone containing predominantly middle Eocene nannofossils and diatoms mixed with rare early Miocene nannofossils and diatoms. Less than 2 m of Campanian–Maestrichtian (Core 19) limestone may or may not also be displaced; this limestone is the last marine sediment recovered above igneous basement.

Calcareous nannofossils are rare and poorly preserved in the Pleistocene–Pliocene mudstones; assemblage preservation and abundances improve within the early Miocene sediments. Nannofossil preservation varies considerably within the angular lithic clasts present within the early Miocene, but species are often age diagnostic of the Oligocene, middle Eocene, and Late Cretaceous. Diatom preservation is relatively poor at this site, but reliable Pleistocene and Pliocene indicators are present. Middle and lower Miocene sediments contain few diagnostic diatom species, which makes confident interpretation of the thanatocoenosis difficult. Benthic foraminifers are few and are moderately preserved in the Pleistocene–Pliocene mudstones, well preserved and abundant within early Miocene sediments, and abundant but recrystallized within the Late Cretaceous limestone. Nannofossils and benthic foraminifers are usually in age agreement for the youngest age represented in a mixture of brecciated lithologies.

Ecologic analysis of the benthic foraminiferal assemblages suggests that water depths were near or below 4000 m throughout the fossiliferous portion of the Tertiary section. Transported specimens are from the shelf and upper bathyal biofacies (core catchers of Cores 3 to 5) and from the slope (core catchers of Cores 8 to 13). Tropical shallow-water species were transported into the abyssal biofacies during the early Miocene. The poorly preserved or barren cores (567A-6 and -7) may have been deposited below the foraminiferal CCD (calcite compensation depth) or may have been effected by corrosive bottom waters. The Cretaceous faunas suggest deposition occurred in the lower slope or equivalent depths on the ocean floor and above the CCD.

Sediment accumulation rates uncorrected for compaction are approximated for both Holes 567 and 567A (Fig. 5). A minimum rate of 40 m/m.y. was determined for the Pleistocene sediments in Hole 567. This is in general agreement with accumulation rates (55 m/m.y.) for the Pleistocene section cored at Site 494. Accumulation rates for the Pliocene sediments cored in Hole 567A

are low in comparison, approximately 8 m/m.y. and may be indicative of an unconformity near the Pliocene/Pleistocene boundary. An unconformity occurs between the early Pliocene and early Miocene at about 220 m. Sediments from 220 to 368 m are assumed to have been deposited during the early Miocene with accumulation rates of approximately 76 m/m.y. This rate is comparable to early Miocene sedimentation rates (100 m/m.y.) for Site 496, which was drilled 20 km north on the mid-Trench slope.

### Calcareous Nannofossils

Calcareous nannofossils occur in rare, poorly preserved numbers within the Pleistocene–Pliocene sediments of both Holes 567 and 567A. Assemblage preservation and diversity improve and abundance increases markedly within the lower Miocene sediments. Species preservation and abundance fluctuate from overgrown or etched rare occurrences to moderately preserved common abundances within the Oligocene, middle Eocene, and Upper Cretaceous angular lithic fragments.

### Hole 567

On the basis of the occurrence of small *Gephyrocapsa* spp. and *G. oceanica*, 567-H1, CC (wash core) is Pleistocene. A mixture of middle to late Miocene species such as *Catinaster coalithus* and *Sphenolithus heteromorphus* also occur, which indicates that Miocene reworking was active in the Pleistocene.

Sample 567-1, CC contains rare *Discoaster brouweri* and *Calcidiscus macintyreii*; and 567-2, CC contains only small *Gephyrocapsa* spp. Both cores are assigned to the early Pleistocene (probable *Calcidiscus macintyreii* Zone) and are very close to the Pleistocene/Pliocene boundary.

### Hole 567A

A sparse nannofossil assemblage with consistent *Reticulofenestra pseudumbilica* and *Sphenolithus neobabes* occurs in Samples 567A-1-4, 50 cm through 567A-3-6, 29 cm. Species typical of the early Pliocene such as *Calcidiscus macintyreii*, *Discoaster pentaradiatus*, and *Discoaster asymmetricus* are present and mixed with rare reworked middle to late Miocene species such as *Discoaster* cf. *bollii* and *Catinaster coalithus*. This interval is assigned to the early Pliocene. Sample 567A-3-6, 32–33 cm contains long-ranging species whose age could be Miocene to early Pliocene.

Sections 567A-3, CC through 567A-10 are assigned to the early Miocene *Helicosphaera ampliaperta* Zone and contain such age diagnostic species as *H. ampliaperta*, *H. mediterranea*, *H. scissura*, *Sphenolithus heteromorphus*, and *Discoaster deflandrei*. The unconformity between the lower Pliocene and lower Miocene sediments therefore lies between 567A-3-4, 28–29 cm, and 567A-3, CC, at approximately 220 m sub-bottom depth, which is in general agreement with paleontological results from Site 494 (basal Pliocene unconformity at 225 m). Early Miocene sediments (*H. ampliaperta* Zone) were also encountered in Hole 498A 3 km west along strike of the lower Trench slope, 50 km north in the upper slope area penetrated at Site 496, and approximately 80 km



Core		Age	Biostratigraphy			Paleo-bathymetry				
Hole 567	Hole 567A		Nannofossil zones or age	Diatom zones	Benthic foraminifers	Neritic	Bathyal			
							Upper	Middle	Lower	Abyssal
H1		early Pleistocene	<i>Calcidiscus macintyre</i>	<i>Pseudoeunotia doliolus</i>	Pleistocene					
1										
2	H1									
	1	early Pliocene	<i>Reticulofenestra pseudoumbilica</i> — <i>Amaurolithus tricorniculatus</i>	<i>Nitzschia jouseae</i>	Pliocene					
	2									
	3									
	4	early Miocene	<i>Helicosphaera ampliaperta</i>		early Miocene					
	5									
	6									
	7			middle to early Miocene	early Miocene					
	8									
	9									
	10									
	11									
	12									
	13									
	14		<i>Helicosphaera ampliaperta</i> <i>Sphenolithus belemnus</i> early Maestrichtian late Campanian	early Miocene	Late Cretaceous					
	15									
	16									
	17									
	18									
	19									
	20									
	21									
	22									
	23									
	24									
	25									
	26									
	27									
	28									
	29									
	30									
	31									
	32									
	33									

Figure 4. Biostratigraphic and paleoecologic summary of Holes 567 and 567A. (Hachures indicate barren intervals.)

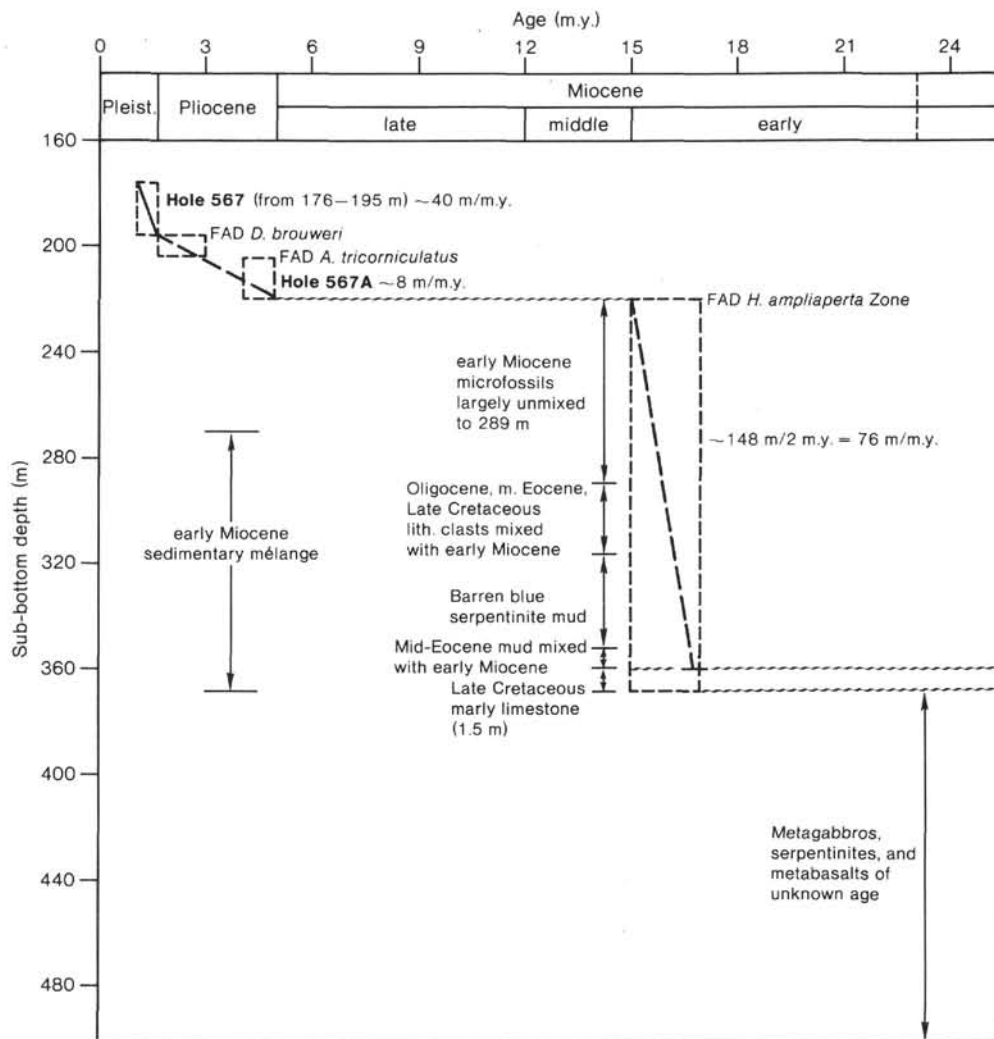


Figure 5. Sediment accumulation rates for Holes 567 and 567A uncorrected for compaction.

north on the shelf edge as documented by the Esso Petrel Well (Seely, 1979). Early Miocene nannofossil species were not reported at Site 494.

Cores 567A-11 through 13 consist of a mixture of angular clasts of variable lithology that contain moderately preserved Oligocene, middle Eocene, and Late Cretaceous nannofossil assemblages in association with an early Miocene mud matrix. In many cases interformational conglomerates of angular lithic clasts in a coherent matrix (see Lithostratigraphy section) can be observed, which would suggest that the angular clasts were emplaced because of slumping or other types of downslope movement and are genetically part of sedimentary breccia. The youngest age obtained from the clasts or matrix would then represent the true age of deposition.

Discrete angular lithic clasts and matrix (often obscured) were selectively sampled to determine the upper and lower limits of age spread. Results are tabulated in Figure 6 and indicate that reworking of an Oligocene-middle Eocene clast occurred as high as Section 567A-7-2, whereas the first reworked Late Cretaceous material was observed in Section 567A-8-4. The age of matrix and some clasts from the lower part of Sections 567A-8-

4 to 567A-10, CC is early Miocene. Clasts from Cores 11 and 12 are Oligocene and Late Cretaceous (probable Campanian), whereas clasts from Core 13 are primarily middle Eocene or Late Cretaceous. Matrix mudstone from Sample 567A-13-2, 20–21 cm contains Oligocene-Cretaceous nannofossils, whereas soft mud (possible matrix) from 567-11, CC, 567A-12, CC, and 567A-13, CC consistently yielded a youngest nannofossil age of early Miocene—the *Helicosphaera ampliapertura* Zone. Deposition would then have taken place in the early Miocene, with erosion, mass transport, and redeposition of subaerially exposed Oligocene through Late Cretaceous sediments as coherent lithic clasts.

Cores 567A-14 through 567A-17, CC recovered weathered blue serpentinite mud, which may or may not be of equivalent age to the blue mud sequence recovered at Site 494 (225–245 m sub-bottom). Both blue mud sequences are barren of nannofossils.

Sample 567A-18-1, 49 cm contains *H. ampliapertura*, *H. kamptneri*, and *Triquetrorhabdulus milowii* along with scattered Cretaceous and Eocene species, and is assigned to the early Miocene *Sphenolithus belemnos* through *Helicosphaera ampliapertura* Zones.

Sample (core-section, interval in cm)	Lithology	Description	Age
6-4, 100–101	Gray mudstone	Angular clast	Miocene (1 cm)
6-4, 100–101	Gray mudstone	Matrix	Miocene
7-2, 11–12	Hard blue green mudstone	Angular clast (1 cm)	Oligocene— mid. Eocene
8-4, 46–47	Gray mudstone	Small clast (5 mm) with matrix	Mixed: Clast— Late Cret. Matrix— early Miocene
8-4, 78–79	Gray mudstone	Matrix	early Miocene
8-4, 81–82	Gray mudstone	Brecciated bedded layer (~1 cm thick)	early Miocene
10-2, 18–19	Light gray mudstone	Brecciated bedded layer (1–2 cm thick)	early Miocene
11-1, 72–73	Gray mudstone, mottled	Matrix with small (1 mm) clasts	Oligocene
12-4, 9–11	Soft blue mudstone	Clast	late Campanian —Maest.
12-5, 44–45	Soft white limestone	Clast	late Campanian —Maest.
13-1, 70–71	Firm, dark brown mudstone	Angular clast (1 cm)	middle Eocene
13-1, 104–110	Gray brown mudstone	Angular clast (1 cm)	middle Eocene
13-1, 147–148	Gray limestone	Angular clast (~5 cm)	Cretaceous
13-2, 20–21	Soft gray mud	Matrix	Mixed: Oligocene—Cret.
13,CC	Soft gray mud	Matrix	Mixed: early Miocene— Late Cretaceous
18,CC	Soft green mudstone	Clast	middle Eocene
18,CC	Soft white mudstone	Clast	Late Cretaceous
18,CC	Soft gray mudstone	Possible matrix underlying serpent- inite mud	Mixed: middle Eocene with rare early Miocene

Figure 6. Nannofossil age determinations of selected lithologies from Hole 567A, Cores 6 through 18.

The base of the blue serpentinite mud is in 567A-18,CC, overlying 6 cm of soft gray mudstone that contain traceable bedded layers truncated by an apparent erosional contact. Lithic clasts within the serpentinite mud were selectively examined for nannofossils and were either middle Eocene or Late Cretaceous. The soft gray mudstone below the serpentinite mud contains a middle Eocene flora along with very rare early Miocene specimens of *H. ampliaperta*, which once again is indicative of an early Miocene sediment dominated by reworked material.

Core 19 recovered 1.5 m of marly limestone that contains moderately recrystallized species of Late Cretaceous nannofossils. The presence of *Broinsonia parca*, *Micula staurophora*, *Tetralithus aculeus*, and *T. gothicus* is indicative of the late Campanian–early Maestrichtian for this sediment as sampled throughout Sections 567A-19-1 and 567A-19,CC and represents the last recovered marine sediment overlying igneous basement.

Cores 20 through 29 recovered gabbro conglomerates, serpentinites, and metabasalts that are of course barren of *in situ* nannofossils. Blue serpentinite mud was examined throughout this interval to determine the extent

and stratigraphic level of downhole contamination. Very rare Tertiary species were observed in Sections 567A-20-1 and 567A-24,CC, which indicates downhole sluff is minimal and not concentrated from a particular horizon.

### Diatoms

Diatom preservation, on the whole, is fair to poor, with intervals—Cores 5 and 6 and Cores 13 through 17—barren of diatoms. There are however, a sufficient number of species present to make a limited number of age interpretations.

Hole 567 was cored entirely within the Pleistocene, as determined by the presence of the marker fossils *Pseudoeunotia doliolus* and *Rhizosolenia praebergonii*.

The first two cores from 567A contain a flora characteristic of the Pliocene, including *Rossiella tatsunokuchiensis*, *Coscinodiscus perforatus*, *Goniothecium odontella*, *Nitzschia jouseae*, *Coscinodiscus nodulifer*, and *Thalassiosira convexa*.

A probable age of middle Miocene is assigned to Sections 567A-7-1 through 567A-13,CC because of the presence of *Bogorovia veniamini*, *Thalassiosira burckliana*, *Craspedodiscus coscinodiscus*, and *Synedra jouseana*.



Core catchers of Cores 12 and 13 contain a different flora, including 12 species not previously encountered. Among these species are *Trinacria excavata* (Eocene–Oligocene), *Melosira clavigera* (late Eocene), *Cyclotella hanae* (Eocene–Miocene), and *Bogorovia veniamini* (late Oligocene–mid-Miocene). Because these samples are sparse and poorly preserved, it is likely that this interval represents a period such as late Oligocene–early Miocene when the thanatocoenosis was possibly composed of secondarily deposited Eocene diatoms. Below this level, diatoms are not present at all again until the core catchers of Cores 18 and 19, where sparse Eocene species occur mixed with the robust Miocene *Craspedodiscus coscinodiscus*, again suggesting a Miocene site of reworked Eocene material.

### Benthic Foraminifers

Rare to common benthic foraminifers were recovered from Holes 567 and 567A. Preservation ranges from the well preserved to poorly preserved. Pleistocene, Pliocene, early Miocene, and Late Cretaceous assemblages were identified. The Oligocene species are rare and probably from reworked lithologic clasts contained in the early Miocene sediments.

Foraminiferal assemblages from Hole 567 contain rare to few poorly preserved foraminifers and are Pleistocene considered to be on the basis of the presence of various bolivinid, uvigerinid, and cassidulinid species. These species also indicate deposition occurred in the lower bathyal to abyssal biofacies, 2000 to 4000 m. The abundance of transported specimens may be related to a lower stand of sea level during increased glaciation.

Benthic foraminifers from Hole 567A range from Pleistocene to Late Cretaceous. Unconformities are noted between the early Pliocene and early Miocene strata and probably between the early Miocene and Late Cretaceous. The age relationship of the strata associated with the latter unconformity is unclear because of the reworked faunas and lithologies, downhole contamination, and barren intervals. Benthic foraminifers in the core catcher of Core 13 are early Miocene to late Oligocene. Foraminifers from selected lithologies stratigraphically higher in the core are as old as middle Eocene to possibly Oligocene. The next fossiliferous core (567A-19, CC and 567A-19-1, 77–79 cm) contains a Late Cretaceous foraminiferal assemblage.

Environmental analysis of the Hole 567A faunas suggests deposition occurred in the abyssal zone ( $\geq 4000$  m) during the Pliocene, with the bulk of the transported specimens derived from the outer shelf and upper bathyal facies. Well-preserved Miocene assemblages in Cores 3 through 5 and 8 through 13 indicate that deposition occurred in the abyssal and lower bathyal facies (2000–4000 m). Shelf and upper-slope specimens were commonly transported in the early Miocene above the barren core catchers (of Cores 6 and 7). Below this level, transported material is primarily from the middle and lower slope.

Ecologic analysis based on the Cretaceous assemblages (Core 19) is not as refined as that for the Tertiary assemblages. The calcareous fauna indicates that deposition occurred above the CCD and probably on the slope or

equivalent depths on the ocean floor. The abundance of planktonic specimens suggests deposition was on the lower slope. Benthic foraminiferal species present are most commonly found in the lower-slope facies (Sliter, 1968, 1977). Depth boundaries are not given for these assemblages.

## PHYSICAL PROPERTIES

### Methods

Measurements of bulk density, wet-water content, porosity, compressional wave velocity, and thermal conductivity were performed as discussed for previous sites of this leg. In addition, some shear strength, penetrometer tests were made, however, these do not represent a systematic sampling of the true sedimentary sequence. Sampling was done on least-disturbed sections in unindurated sediment, some serpentinite muds, and principally on discrete clasts or pieces of indurated material.

### Results

The physical properties for this site reflect the variable lithologies encountered, mainly mudstone, serpentinite in various degrees of weathering, limestone, and igneous basement. Bulk density, wet-water content, and porosity are shown in Figure 7, where bulk density reflects a mirror image of the other two properties. The bulk density of mudstone samples varies around an average of  $1.70 \text{ Mg/m}^3$  and porosity averages about 55% in the section between 201 and 281 m sub-bottom. Deviations resulting from limestone and serpentinite conglomerate horizons occur through this zone. Below 281 m the dominating lithologies are reflected by the significantly higher bulk densities and corresponding lower porosities.

Sonic velocity and acoustic impedance measured perpendicular to the bedding plane are displayed in Figure 8. The evident lithologies show discrete ranges in physical property characteristics as depicted in Table 2. Notice should be given to the range of serpentinite material, which varied from a serpentinite flour to hard rock.

A few measurements of thermal conductivity were made on half round slabs without polishing the surface of these slabs (Table 3). These data are not corrected to *in situ* conditions and represent approximations because of questionable probe contact with the samples.

### Discussion

Lithostratigraphic and biostratigraphic observations of the sediment character at this site reveal a high degree of incorporated clasts in mudstone matrix. Interpretation of the history of the sediment as reflected by physical properties becomes extremely difficult under such conditions, because sampling is limited to discrete pieces of undisturbed material. Mass movement certainly plays a major role in the deposition of the recovered sedimentary sequence and is responsible for the consolidated and homogeneous nature of the mudstone. Fractures within the basement rock and the interbedded nature of serpentinite mud suggest that basement has undergone strain related to external stressing. The serpentinite mud, having higher water contents and permeabilities, most

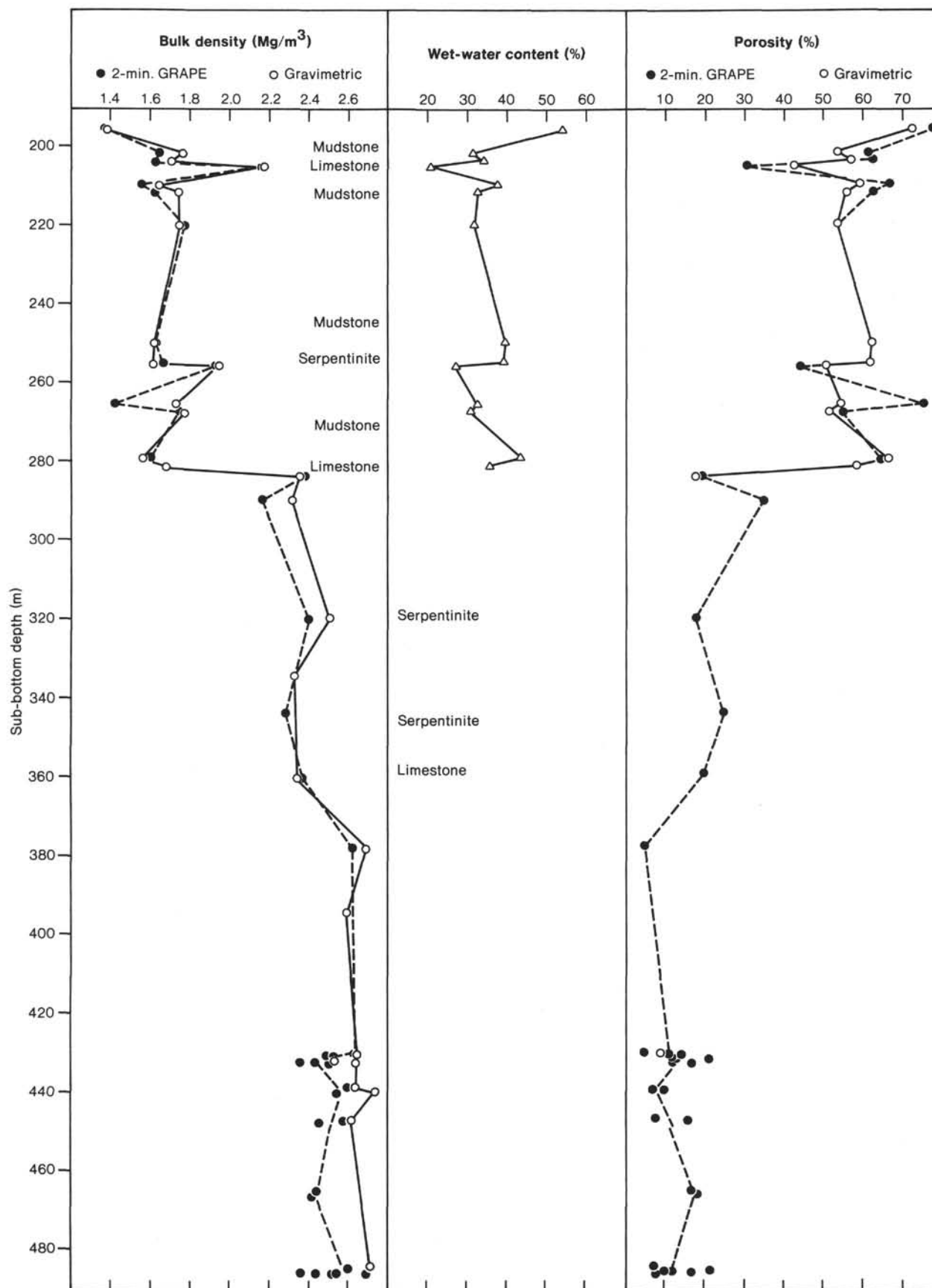


Figure 7. Index properties of sediments and rock at Hole 567A.

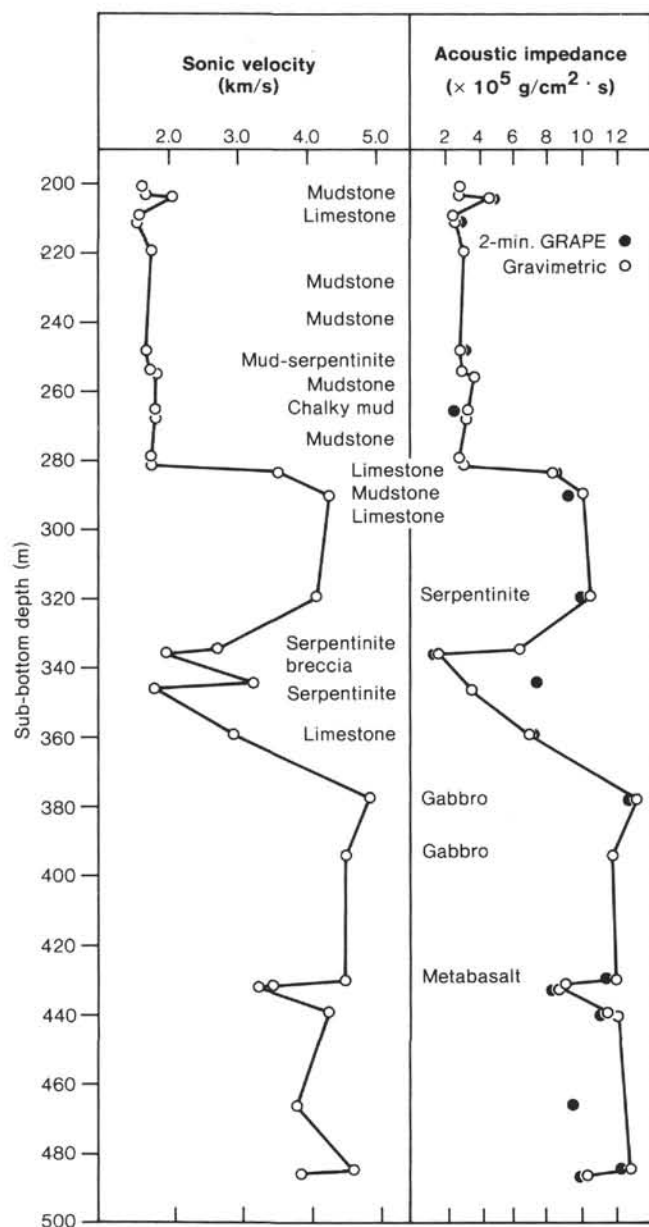


Figure 8. Acoustic characteristics of sediments and rock at Hole 567A.

Table 2. Range of physical properties for major lithologies, Hole 567A.

Lithology	Bulk density (Mg/m <sup>3</sup> )	Porosity (%)	Sonic velocity (km/s)
Mudstone	1.39–1.77	51.9–77.7	1.54–1.78
Limestone	2.11–2.37	17.8–42.3	2.03–4.31
Serpentinite	1.87–2.50	17.9–50.7	1.75–4.10
Igneous basement	2.36–2.70	4.2–20.5	3.21–4.82

likely represents the slip planes of any movement within this zone.

### Downhole Logging

Caliper, gamma-ray, sonic velocity, self potential, resistivity, formation density-compensated, and neutron porosity log passes were made between the interval of 66

Table 3. Thermal conductivity of sections from Hole 567A.

Section	Sub-bottom depth (m)	Thermal conductivity (mcal/cm°C · s)
567A-16-1	334.20	6.681
567A-25-1	430.20	4.600
567A-25-2	432.10	10.022
567A-26-1	439.00	7.385

and 276 m sub-bottom. Bridging at the base of the interval limited logging, and the subsequent loss of the drill string eliminated the possibility of further work. The caliper log shows that the logged interval was essentially a wide open hole, and identification of washed section is revealed principally in gamma-ray, neutron porosity, and formation density log records.

The logged interval shows a very homogeneous section corresponding most likely to the mudstone section, with bulk densities averaging between 1.55 and 1.75 Mg/m<sup>3</sup>, porosities between 50 and 75%, and sonic velocities on the order of 1.7 to 1.8 km/s. These values correspond to within 5% of the range obtained by laboratory measurements of physical properties. The log also reflects the homogeneous nature revealed in Figures 7 and 8 between 200 and 280 m sub-bottom, suggesting the nature of washed material above 200 m is indeed the mudstone facies. In addition, the log agrees with the measured physical properties at Site 494 for this interval, composed of mud and mudstone facies.

Two horizons with distinct characteristics are found at 113 and 254 m sub-bottom. These two units have a bulk density of approximately 2.1 Mg/m<sup>3</sup>, porosity of 52%, and sonic velocities near 2.0 to 2.4 km/s. The horizon at 254 m corresponds to a mudstone-serpentinite conglomerate that shows contrasting physical properties with the overall section, although the laboratory measurements do not reveal the extremes obtained by logging. This discrepancy may result simply from disturbance of recovered material during coring. Nevertheless, the possibility of a similar conglomerate horizon at 113 m exists, and both of these may produce reflectors observed in the seismic record.

The resistivity record shows some slight deviations occurring at 5715, 5733, 5746, and 5763 m (186, 204, 217, and 234 m sub-bottom). The sonic log also shows a shift to an almost constant 1.6 km/s at these same intervals. These slight deviations may be a response to thin open conglomerate horizons, as suggested by recovery of a limestone clast at 204 m. Physical properties of this clast cause the deviation shown at this depth in Figures 7 and 8. This correlation is based on a weak response from logging tools and recovery from one core. Unfortunately, the other cored intervals recovered brecciated material, therefore this correlation is tenuous.

### GEOPHYSICS

Site 567, at the foot of the landward slope of the Middle America Trench off Guatemala, is about 3 km up-slope and 550 m above the level of the Trench floor. Hole 567A is within 110 m of Site 494 drilled on Leg 67.



Two generations of geophysical work have been done around Site 567. The first was prior to drilling on Leg 67, when the University of Texas made a site survey that was the primary data for that leg. From this and some previous studies based mainly on geophysics, an orderly constant accretion of sediment was proposed as the principal tectonic mechanism that formed the slope. However, the sediment section at Site 494 required another quite different explanation, so further geophysical work became important. As part of the second generation of geophysical work, some University of Texas data were processed further, a limited Seabeam study was undertaken, and a deep-tow study was made. In this section the results of post-Leg 67 geophysical work are described; the reader is referred to the following papers for a more comprehensive and historical treatment of the geophysical data at Site 567, which is essentially a further drilling of Site 494 (Leg 67): Seely et al., 1974; See-

ly, 1979; Ibrahim et al., 1979; Ladd et al., 1982; von Huene et al., 1982; Moore et al., 1982).

The detailed bathymetry obtained by the Seabeam instrument aboard the *J. Charcot* (Aubouin, et al., 1981) shows the complexity of bathymetry on the first of three benches (the 494 bench) above the Trench floor (Fig. 9). The benches off Guatemala occur mainly on the IPOD transect. Rather than simple back-tilted benches with ponded sediment, as commonly noted on the landward slopes of trenches, the fine-scaled topography of all three benches off Guatemala is marked by isolated highs and closed lows as well as obliquely transverse trends. There is much small-scale disorganized topography rather than systematic long narrow basins and ridges. The steep slopes between benches are less regular than the straight escarpment at the foot of the landward slope of the Trench, despite the intersection of oblique trending ridges with the escarpment. A remarkable aspect of the

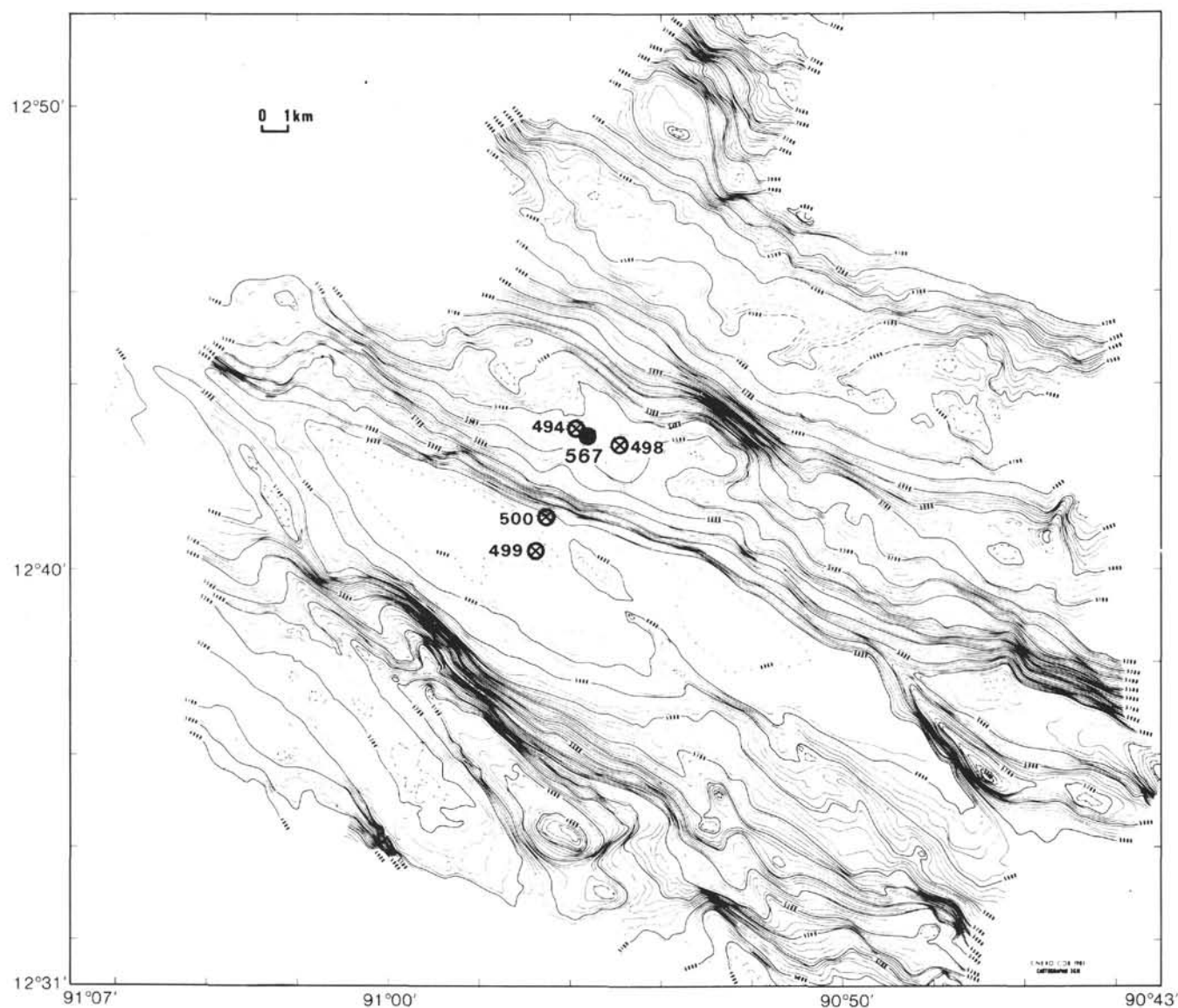


Figure 9. Bathymetric map made with the Seabeam instrument aboard the *J. Charcot* (from Aubouin et al., 1981).

map is the indication that subducting ocean ridges are accommodated by the landward slope of the Trench with very little disruption of the topography of the Trench-slope juncture. Site 567, on the lowest bench, is about 550 m above the Trench floor and is close to the projection of a linear ridge on the ocean crust that stands about 200 m high but protrudes only about 50 m above the sediment ponded in the Trench. If there were much coupling across the subduction zone, abundant compressional structures should mark the tectonic setting of the bench and should be seen in Site 567 cores.

Deep-tow records bracket the site with lines both parallel and perpendicular to the slope (Fig. 10). The deep-tow instrument's 4.5-kHz transducer penetrated up to 100 m deep in sediment on the lowest bench. Most folds and faults have no surface expression in the 4.5-kHz records nor on the sidescan sonar records. From their generally equal distribution along orthogonal trending records, the structures appear to strike both parallel and transverse to the slope, and extend laterally for 1 km or less. The sediment in which the structures are seen is up to 1 m.y. old, as based on the 100-m/m.y. accumulation rates at Site 494 (Aubouin, von Huene, et al., 1982).

Seismic record GUA-13 (Ladd et al., 1982), the basic line for the Guatemalan transect, was redisplayed with scaling parameters that emphasize the shallow detail more (Fig. 11). A few reflections have been highlighted in Figure 13, and some are keyed by letters (Fig. 11) to the lithology at Site 567 using velocities from refraction measurements, laboratory velocities, and logging (Figure 12).

Velocity data are taken mainly from measurements on samples and a short logging run in the mudstone section (see Physical Properties section). Logs could not be run in the serpentinite and ophiolite, which left minimum uncertainties of about 600 m/s for the last 150 m of the drilled section and the undrilled reflections below. The average of 6 measurements in weathered and sheared serpentinite is  $2.13 \pm 0.6$  km/s, and the average of 11 measurements in peridotite, gabbro, and basalt is  $4.2 \pm 0.5$  km/s. If these velocities are weighted in proportion to the lithologies recovered in the igneous section from 358 to 501 m (48% serpentinite and 52% igneous rock), the section velocity is 3.2 km/s; if weighted by lithology derived from drilling rate (26% serpentinite, 74% igneous rock), the section velocity is 3.7 km/s. The former is most consistent with refraction measurements in the

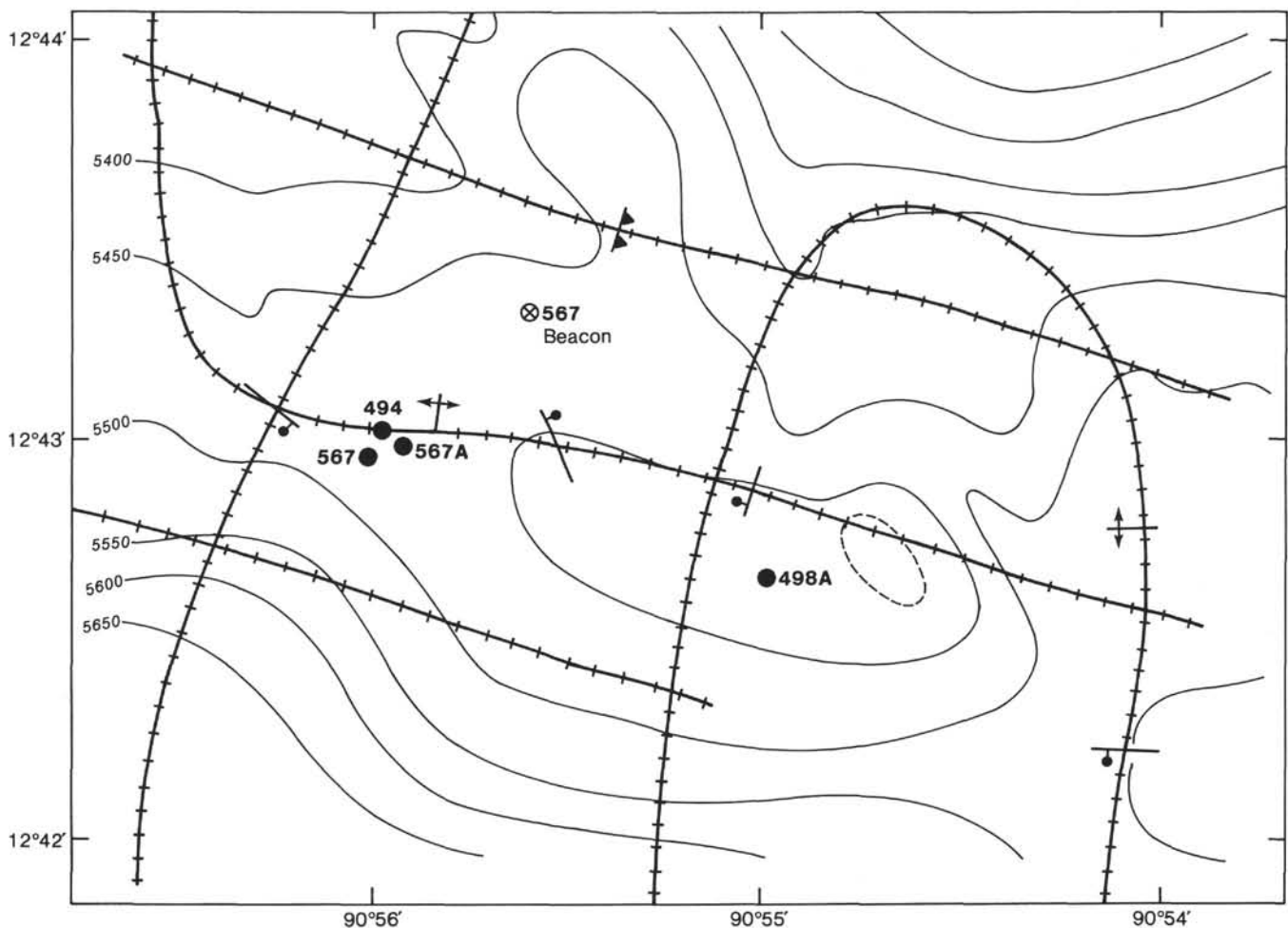


Figure 10. Sketch map of the deep-tow survey around Sites 494, 498, and 567. Track lines are shown with small hachures, contours in solid lines are at 50-m intervals. All structures are shown with strike perpendicular to track lines unless otherwise indicated. From unpublished work in progress by G. Moore and P. Lonsdale (personal communication, 1981).

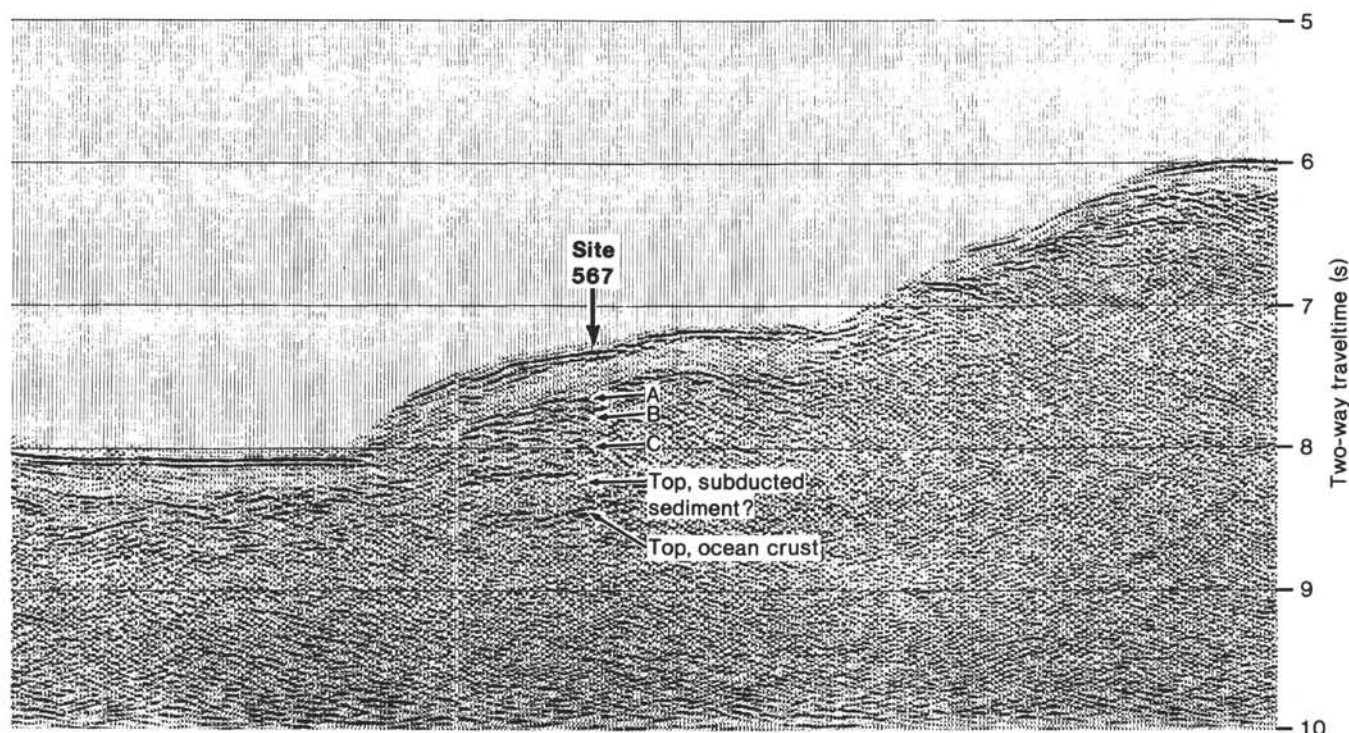


Figure 11. Reprocessed seismic record including migration showing reflections A, B, C, and possible top of subducted sediment. Site 567 was drilled to approximately reflector C.

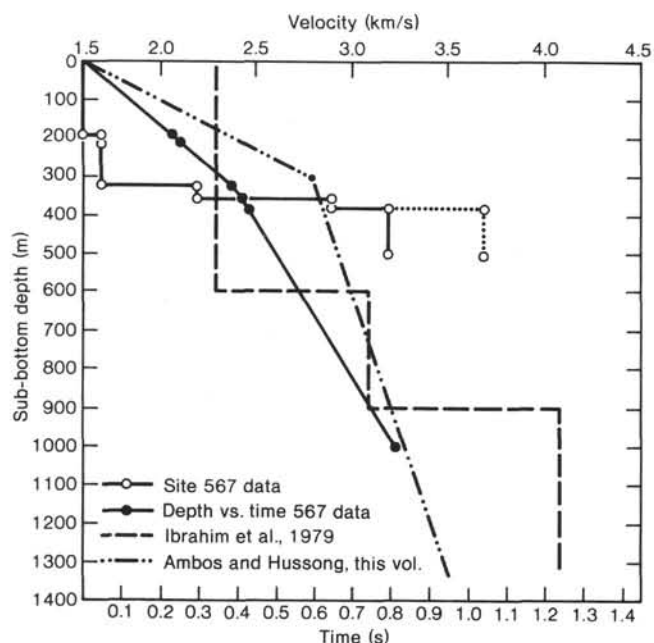


Figure 12. Seismic velocities at Site 567 determined by OBS refraction methods (Ibrahim et al., 1979; Ambos and Hussong, this volume) and from core and downhole logs run at Site 567. Note that a depth-time plot based on the Site 567 data is also included.

area (Fig. 12), although the latter seems a better way to average the section velocity; the former is used in making the following estimates of depth in the reflections of Figure 11: reflection A—320 m, top of serpentinite at

325 m; reflection B—352 m, contact of serpentinite and limestone at 359 m; reflection C—490-m diffractions, possibly from top of deformed rock at the top of the subduction zone.

A sketched depth section (Fig. 13) of the 494 bench was made using velocities measured at Site 567. Reflections A and B are subhorizontal; their departures from a straight line could be caused by faults or folding. Deformation below horizon A is more intense than above, as suggested by steeper dips of reflections. Horizon C has much steeper flanks than shown because it is a diffraction; it may represent the top of the ridge being subducted as seen in the Seabeam map (Fig. 9) or the top of the deformed zone associated with the subduction zone.

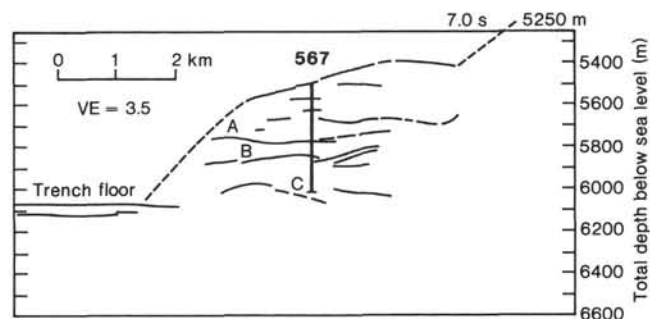


Figure 13. Depth section showing selected reflections from Figure 11. Velocities used are those from the Site 567 data as shown in Figure 12.

The approximate depth of the igneous ocean crust could vary by hundreds of meters from the position shown.

Interpretation of these geophysical data is preliminary, because not all of the processing was accomplished prior to the cruise. The internal structure at the foot of the slope of the Trench is generally subhorizontal. These horizons appear to project to the slope where they may crop out, however, the deep-tow data do not reveal a rugged slope indicating truncated horizons. Thus at least a thin veneer of sediment must cover the truncated end of the lithologic sequence at the foot of the slope. The depth section is necessarily oversimplified and faults can be drawn across the interpreted horizons, but none with more than 100 to 200 m vertical displacement. Nonetheless, the small number of faults on the deep-tow records and the lack of major fault scarps in the Seabeam data indicate surprisingly little tectonism considering the early Miocene age of the oldest slope deposits covering the basement and their position just 400 to 500 m above the subduction zone. It appears that drilling at Site 567 was terminated just tens of meters above a suspected structure associated with the subduction zone. This is consistent with the drilling difficulty and with the signs of overpressure during the period when the drill stem was stuck. When the pumps were shut off during the operation to free the stuck drill string, a 520 psi pressure remained. If the stuck bottom-hole assembly was sealed off sufficiently to prevent the counterflow of drilling mud and cuttings, then the pressure measurement reflects a formation pressure value that is about 90% of lithostatic pressure.

### Overpressure Observations

Evidence of greater than hydrostatic formation pressure was observed at the bottom of Hole 567A when the drill string became stuck. Just prior to sticking, the pressure read at the surface when circulating 244 gal./min. was 300 to 350 psi. When first stuck, the pressure when circulating at 230 gal./min. was 1000 psi read at the surface. With the pump turned off the pressure decreased to 550 psi but did not go to zero pressure, and when the system was bled to zero, closed, but with no pump, the pressure built up again to 500 psi. Because pumping had no effect on the stuck pipe, it was discontinued for nearly 2 hr. while the stuck pipe was worked to free it. The pressure remained at 500 psi. Once the pipe moved a few feet the pressure dropped to 250 psi and when the pipe came free it dropped to essentially zero.

These observations are explained as follows. The pipe stuck because cuttings collected around the bottom hole assembly and sealed off the bottom of the hole. This caused the pressure to rise to 1000 psi over hydrostatic as measured at the surface, and the water being pumped down the drill stem escaped into the fractured rock. The steady 500 psi for 2 hr. could not have been caused by normal backflow of water and cuttings from up the annulus because the pressure should diminish as the drill cuttings settle out. The drop in pressure to zero after the pipe was freed supports this conclusion. The conditions monitored at the rig floor are similar to those at Site 565 and on Leg 78A at the Barbados Trough, where forma-

tion pressures of 300 psi were reported (Moore, Biju-Duval, et al., in press).

### PALEOMAGNETISM

A limited number of sedimentary samples were taken from cores recovered at the second hole (567A) because of the unconsolidated nature of most of the material. Selected sedimentary samples were subjected to stepwise alternating field demagnetization. The results are plotted in Figure 14. Inclinations are calculated relative to the plane at right angles to each core's axis, whereas declinations are relative to the split faces of the cores. All samples show similar behavior, except the sample from Core 2, which has a reversed inclination. The increase in intensity signifies an overprinted component of opposite polarity. The inclination stabilizes at about  $-43^\circ$ , which is considerably higher than an axial dipole field at this latitude. Although some of this high inclination could be the consequence of secular variation, the result suggests that bedding in this part of Core 2 may be inclined at  $20^\circ$  or more to the horizontal. The higher stability of the normally magnetized samples is possibly the result of overprinting of a normal field component having higher magnetic stability. Data for all the

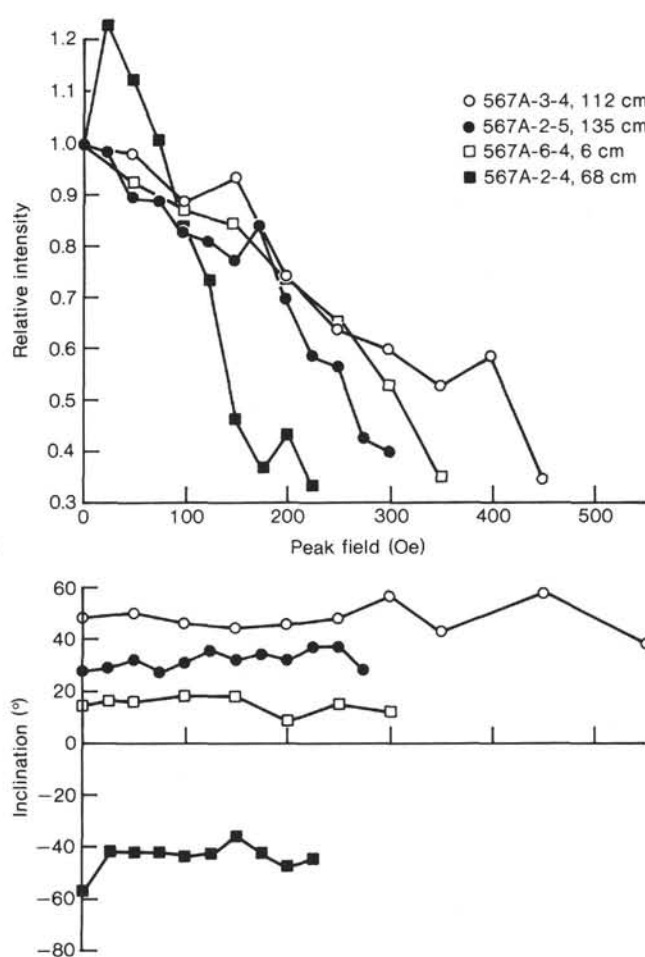


Figure 14. Hole 567A: alternating field demagnetization of selected sedimentary samples.



sedimentary samples after demagnetization at 100 Oe are plotted in Figure 15. All samples except one in Core 2 and one in Core 4 have normal inclinations, with many close to the present field at this site, which has an inclination of  $40^\circ$ . The closeness of the inclinations of almost all these samples to that of the present field is again consistent with normal overprinting.

Serpentinites were encountered in cores 13 to 18. Two serpentinite samples were subjected to stepwise A.F. demagnetization. The results are plotted in Figure 16. Both samples show similar behavior with only small changes in direction up to 400 Oe. The stable inclinations are both close to  $20^\circ$ , which is the expected axial dipole inclination at this site. This implies that the serpentinites have not undergone any significant rotation or north-south movement since emplacement. Shown in Table 4

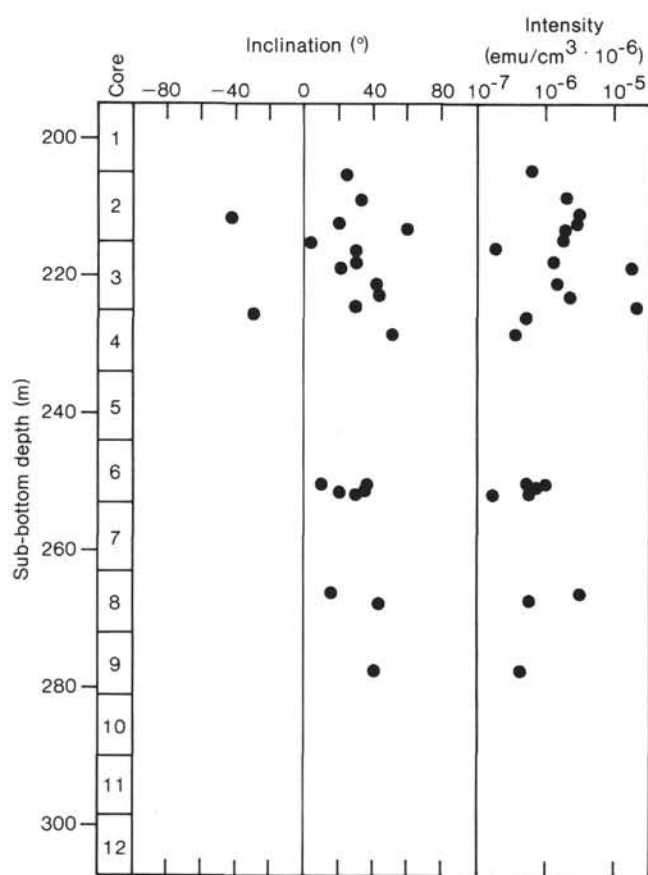


Figure 15. Stratigraphic plot of data for Hole 567A after demagnetization at 100 Oe.

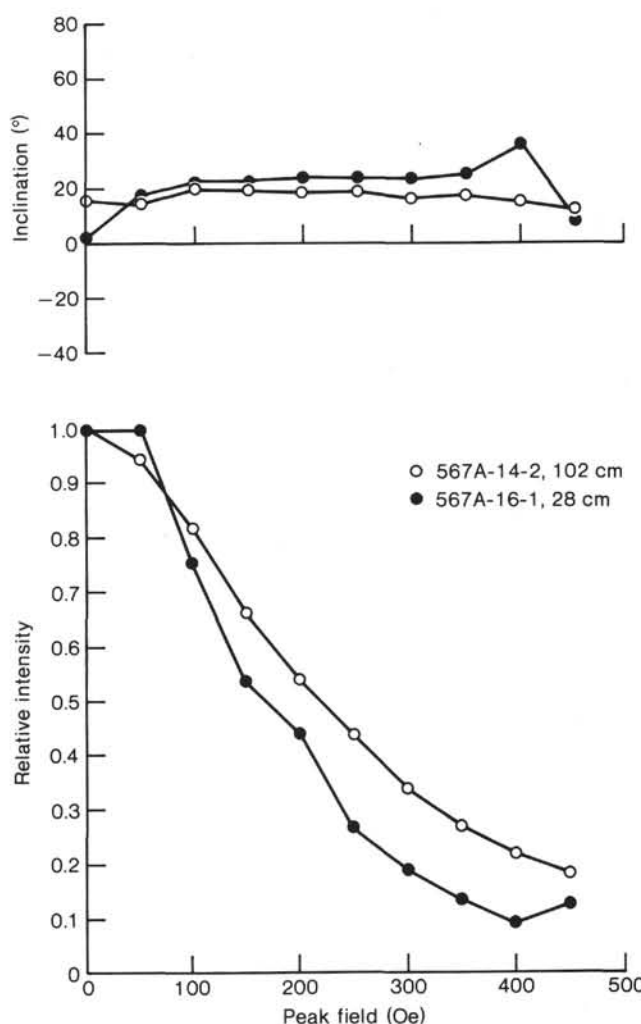


Figure 16. Alternating field demagnetization of serpentinite samples from Hole 567A.

are the susceptibilities and Königsberger ratios,  $Q_n$ , of remanent to induced moment. The susceptibilities are very high ( $10^{-3}$  emu/Oe/cm<sup>3</sup>) and indicate volume percentages of greater than 1% magnetite. However, the low  $Q_n$  (less than 1) values are consistent with the lack of magnetic anomalies in the region surrounding this site.

Upper Cretaceous limestones were encountered in Core 19. Results of stepwise A.F. demagnetization on two samples are plotted in Figures 17 and 18. The plots indicate that small secondary components are removed in fields up to 150 Oe, after which the directions remain

Table 4. Magnetic properties of igneous and metamorphic rocks from Hole 567A.

Sample (core-section, cm level)	NRM ( $\times 10^{-4}$ emu/cm <sup>3</sup> )	Susceptibility ( $\times 10^{-6}$ cm · g · s)	$Q_n$
14-2, 102 cm	6.8	18.4	0.92
16-1, 28 cm	2.8	9.4	0.74
25-1, 37 cm	3.0	25.0	0.30
25-1, 108 cm	4.0	15.0	0.67
25-2, 100 cm	3.1	51.0	0.15
26-1, 52 cm	4.8	11.0	1.10
28-1, 115 cm	12.5	27.0	1.20

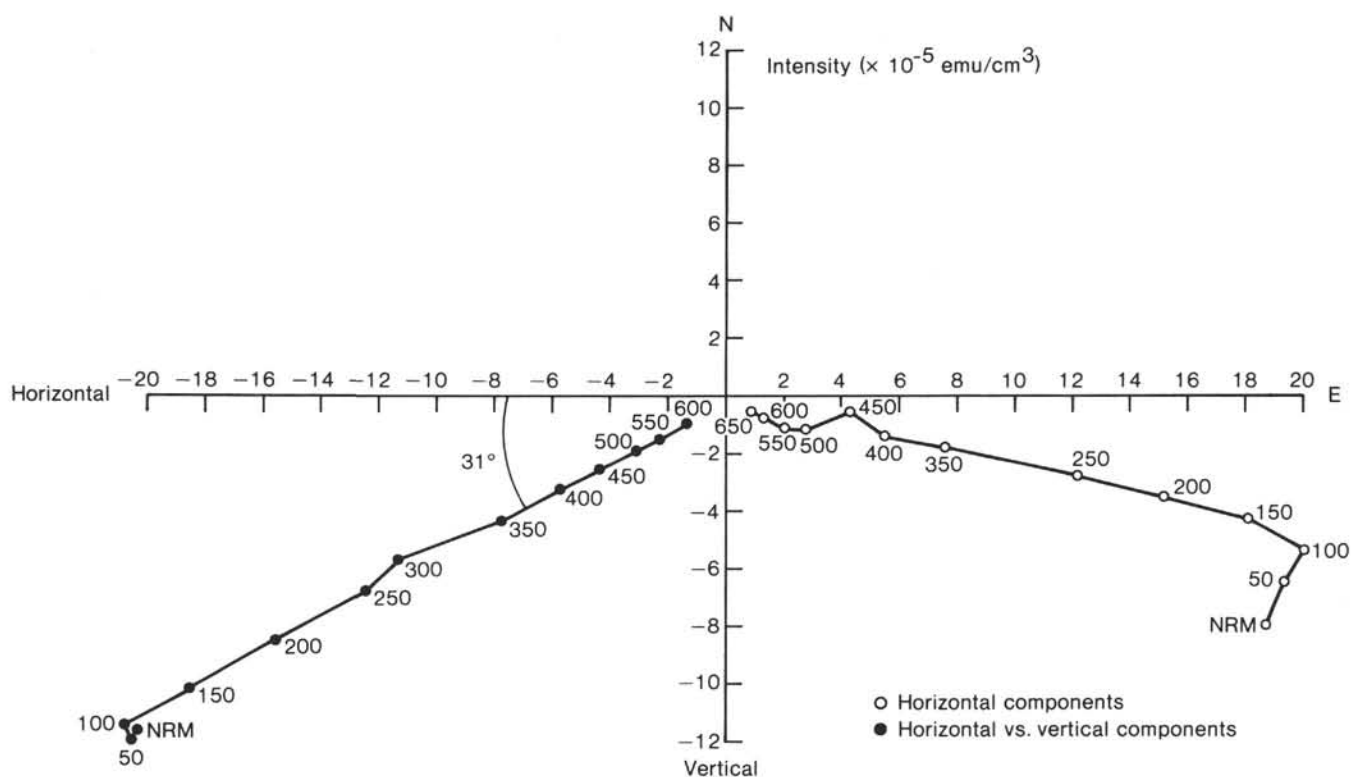


Figure 17. Direction and intensity changes occurring in limestone Sample 567A-19-1, 78 cm during alternating field demagnetization.

very stable up to fields approaching 500 Oe. Sample 567A-19-1, 78 cm has a stable reversed inclination of  $-56^\circ$  relative to the present horizontal, whereas Sample 567A-19-1, 86 cm has a normal inclination of  $31^\circ$ . A bedding correction was applied to the reversed sample based on the dip of observed laminations that were inclined at  $40^\circ$  to the horizontal, with a strike of  $20^\circ$  relative to the split face of the core. The result was an inclination of  $-36^\circ$  relative to the bedding plane. Assuming a dip of  $20^\circ$  for the Cretaceous field, the result indicates that either the bedding was originally inclined at least  $16^\circ$  to the horizontal or that the limestone was formed at a paleolatitude of  $20^\circ\text{N}$ – $10^\circ$  north of the present latitude. This latitude is consistent with previous measurements on Upper Cretaceous samples from DSDP Site 494 (Gose, 1982).

Bedding could not be estimated in the second sample because of its small size. However, the sample is normally magnetized, which may indicate that the reversed sample was formed prior to the normal to reversed transition occurring at the end of the Campanian. This would place the reversed sample in the Late Maestrichtian.

Samples of metabasalt were obtained from Cores 25, 26, and 28. Samples 2.5 cm in diameter were drilled into the split face of core sections in which the vertical direction could be established. Results of stepwise A.F. demagnetization performed on these samples are plotted in Figure 19. One of the samples (567A-25-2, 100 cm) possessed a very high viscous component of magnetization that changed during the course of each spin (about 30 s); this sample clearly has a much lower stability than the other samples (Fig. 19). Two of the samples show a

slight increase in intensity of magnetization up to 150 Oe, which may indicate the presence of an unstable component having opposite polarity. The inclinations, which appear in Table 4, either do not change with demagnetization, or stabilize in fields of 250 Oe. However, the inclination values are different for all the samples, ranging between  $-40^\circ$  for 567A-25-1, 108 cm and  $+60^\circ$  for 567A-26-1, 52 cm. This range indicates that either these samples were magnetized at very different times or they have undergone varying degrees of structural rotation since they acquired their magnetizations. Values obtained for the magnetic susceptibilities and Königsberger ratios ( $Q_n$ ) are shown in Table 4. The susceptibilities are all very high, indicating large-volume percentages of magnetite, greater than 5% for Sample 567A-25-2, 100 cm. Values of  $Q_n$  are all very low, which indicates that these rocks, although they contain more magnetite than the serpentinites, would produce even smaller magnetic anomalies.

## GEOCHEMISTRY

### Gas Analyses

Hydrocarbon gases methane ( $\text{C}_1$ ), ethane ( $\text{C}_2$ ), propane ( $\text{C}_3$ ), isobutane ( $i\text{-C}_4$ ), normal butane ( $n\text{-C}_4$ ), neopentane ( $\text{neo-C}_5$ ), isopentane ( $i\text{-C}_5$ ), and normal pentane ( $n\text{-C}_5$ ) were identified as components of the gases recovered by vacutainers from cores of sediment from Holes 567 and 567A. A single gas sample was recovered by vacutainer from a wash core of Hole 567 representing a sediment interval from 0 to 176.1 m. A high  $\text{C}_1/\text{C}_2$  ratios of about 11,000 suggests that the gases within this

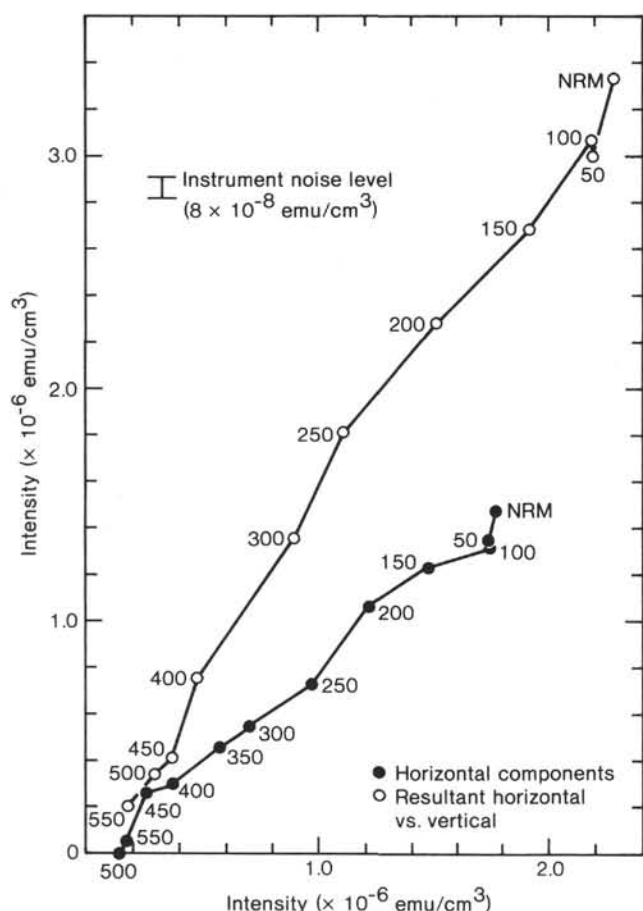


Figure 18. Alternating field demagnetization of basement Sample 567A-19-1, 78 cm.

core were mainly from biogenic sources. Hole 567A started with a wash core representing the sediments from a sub-bottom depth of 0 to 195.5 m. From this wash core a sample of gas was removed by vacutainer. The  $C_1/C_2$  ratio of this gas was about 80,000, indicating, as did the wash core from Hole 567, that the gas came from mainly biogenic sources. Below a sub-bottom depth of 195.5 m, samples of gas were recovered by vacutainers from most cores to the bottom of the hole at 501 m, and these samples were subsequently analyzed by gas chromatography. Results are summarized in Table 5.

Concentrations of  $C_1$  decrease from greater than about 40 to about 1% or less below about 350 m sub-bottom where cores containing mainly ultrabasic rocks and rock cuttings were recovered. These low concentrations result because these rock-containing cores probably had little *in situ* gas present, and the cores did not seal the gas in pockets as occurs with unconsolidated sediment; consequently, the gas concentrations are low and significantly diluted with air.

Ratios of  $C_1$  to  $C_2$  decrease exponentially from 7500 to 3600 in the depth interval from 200 to about 500 m sub-bottom (Fig. 20). Such an exponential decrease in  $C_1/C_2$  ratio is common in oceanic sediment (Claypool, 1976). Below a depth of about 350 m where ultrabasic

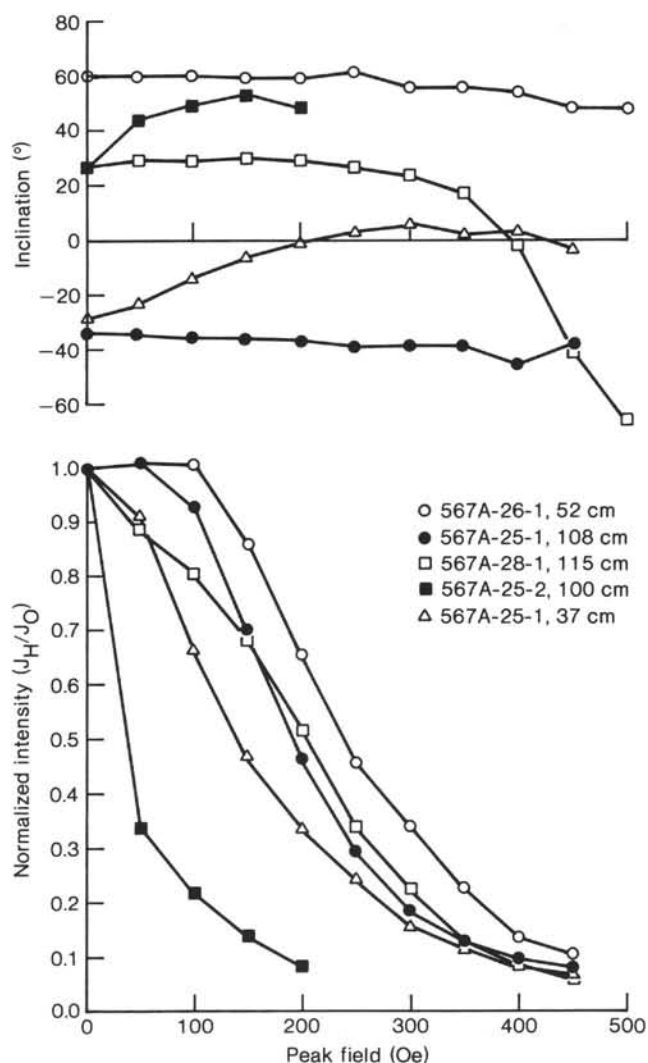


Figure 19. Alternating field demagnetization of basement samples from Hole 567A.

rocks were cored, the  $C_1/C_2$  ratios fluctuated greatly because of the low gas concentrations that cannot be accurately quantified. In Core 19 (360 m) the  $C_1/C_2$  ratio increased by more than an order of magnitude (from 3600 to 60,000), but this high ratio was not measured again in deeper samples.

### Interstitial Water Chemistry

The following inorganic parameters were measured: calcium, magnesium, chlorinity, salinity, alkalinity, and pH. The results are displayed in Figure 21. The increasing values of salinity and chlorinity with depth suggest that gas hydrates have not formed in these sediments. This conclusion is based on arguments presented by Hesse and Harrison (1981) and discussed in the Site 565 report.

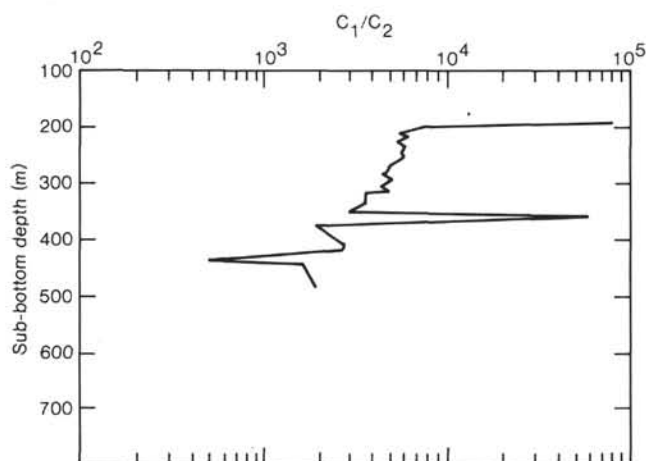
### Summary

1. Below about 200 m at Site 567, hydrocarbon gases are present in all cores containing either unconsolidated sediment or rock. The amount of gas recovered from

Table 5. Distribution of hydrocarbon gases at Hole 567A.

Core-section	Sub-bottom depth (m)	C <sub>1</sub> (%)	C <sub>2</sub> (ppm)	C <sub>3</sub> (ppm)	i-C <sub>4</sub> (ppm)	n-C <sub>4</sub> (ppm)	neo-C <sub>5</sub> (ppm)	i-C <sub>5</sub> (ppm)	n-C <sub>5</sub> (ppm)
1-6	203	77.00	103.00	1.90	1.40	0.30	.75	1.40	0.02
2-5	212	80.00	145.00	2.10	1.60	0.28	1.10	1.40	0.07
3-3	219	76.00	123.00	1.70	1.10	0.20	1.20	1.10	0.02
4-1	225	67.00	128.00	1.40	0.77	0.15	1.10	0.68	0.04
5-3	237	73.00	123.00	1.30	0.62	0.13	1.10	0.61	0.05
6-5	250	49.00	86.00	0.92	0.41	0.09	0.69	0.65	0.03
7-2	255	59.00	103.00	1.10	0.42	0.11	0.86	0.62	0.07
8-4	268	76.00	156.00	1.60	0.63	0.17	1.40	0.78	0.02
9-5	278	77.00	163.00	1.50	0.49	0.13	1.10	0.68	—
10-1	281	2.00	4.50	0.21	0.04	0.01	0.05	0.46	—
11-2	291	30.00	60.00	0.59	0.21	0.02	0.35	0.42	0.10
12-2	301	37.00	83.00	0.89	0.28	0.09	0.72	0.57	0.05
13-4	313	0.47	0.96	0.18	0.03	0.01	—	0.54	—
14-2	319	32.00	89.00	0.55	0.14	0.04	0.88	0.52	0.03
16-2	336	44.00	123.00	0.59	0.16	0.05	1.07	0.48	0.05
17-2	346	66.00	209.00	0.71	0.21	0.06	1.90	0.54	0.05
18-1	352	6.00	21.00	0.61	0.11	0.08	0.40	0.14	0.23
19-1	359	2.00	0.32	0.06	—	—	—	—	—
20-1	377	1.30	6.80	0.62	0.08	0.10	0.30	0.08	0.09
23-1	412	1.20	4.20	0.34	0.05	0.02	0.08	0.09	0.12
24-1	421	13.00	51.00	0.37	0.07	0.03	0.83	0.17	0.08
25-1	430	0.20	2.00	0.30	—	—	0.04	—	—
26-1	438	0.16	3.30	0.36	0.08	0.03	0.08	—	0.10
27-1	446	3.50	21.00	0.37	0.06	0.04	0.24	0.16	0.06
29-2	486	1.30	6.50	0.36	0.06	0.02	0.13	—	0.06

Note: — indicates not detected.

Figure 20. Ratio of methane to ethane (C<sub>1</sub>/C<sub>2</sub>) with depth at Hole 567A.

rock-containing cores was low. C<sub>1</sub>/C<sub>2</sub> ratios decrease exponentially with depth from about 7500 to about 2000.

2. Salinity and chlorinity increase with depth, suggesting that gas hydrates have not formed at this site.

### SUMMARY AND CONCLUSIONS

Site 567 is at the base of the landward slope of the Middle America Trench 3 km upslope and 550 m higher than the Trench floor. It is situated on the first of three benches above the Trench floor and about 110 m from Site 494 drilled on Leg 67. The decision to return to Site 494 was prompted, first, by the failure to complete the drilling on Leg 67 and, second, by the desire to confirm the unexpected results indicating an unusual sequence

of rock in a setting at the front of a convergent margin. Below a Paleogene and Upper Cretaceous sequence, an undrilled section possibly of igneous affinity appeared to rest in turn on subducted Neogene sediment, and drilling was needed to test the unsampled geologic section. The top of the subduction zone was estimated from seismic reflection record GUA-13 (Ladd et al., 1978) at 600 to 800 m depth, a depth well within *Glomar Challenger* drilling capability. The rock below the Cretaceous limestone at Site 567 was found to be of igneous origin and required extensive drilling time; deteriorating hole conditions and bit wear caused termination of drilling perhaps as close as 20 m to the top of the subduction zone in ophiolitic rock. Elevated formation fluid pressure, perhaps from dewatering of subducted sediment, appears to have been encountered at the bottom of the hole.

At Site 567 lithostratigraphic investigations were focused on the part of the record below the Upper Cretaceous marl and limestone recovered at Site 494, however, the Pliocene and Miocene lithologies were cored again to improve on the poor recovery at 494 (Fig. 22). Instead of the normal increase of age with depth as interpreted for Site 494, at Site 567 the Pliocene unconformity is underlain by a 110-m-thick lower Miocene, dark olive gray mudstone with abundant subangular to subround clasts containing Oligocene mudstone, middle Eocene siliceous mudstone, and Upper Cretaceous (Campanian) limestone. At Site 494 these lithologies were thought to be partly reworked and partly in place. At Site 567, there are layers of the distinctive blue gray mudstone that appear to be serpentinitic mud and one bed of serpentinite pebbles. At the base of the next lower unit an 18-m-thick serpentinitic mud, a thin layer of the Miocene mudstone was cored. This relation makes interpre-



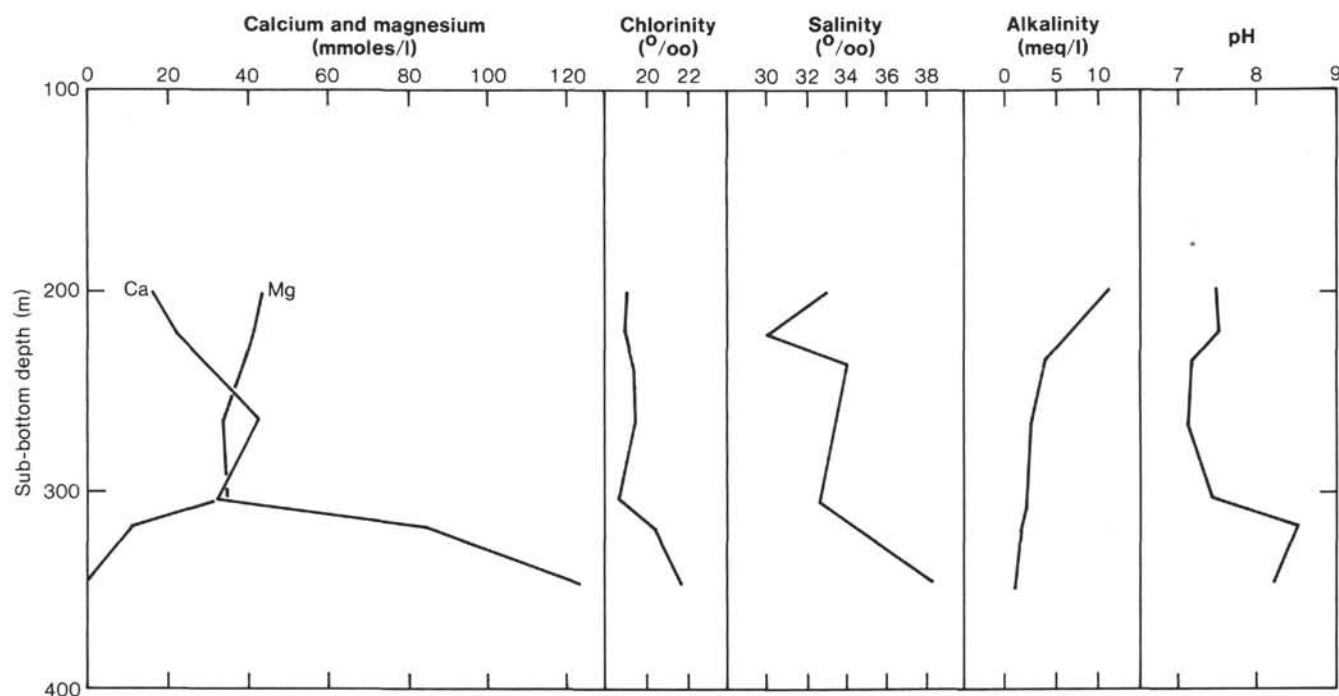


Figure 21. Chemistry of interstitial water at Site 567.

tation of origin somewhat uncertain, although a transported block seems to be the best explanation. Beneath the serpentinite is Cretaceous limestone, the origin of which is also less than certain. The limestone, 20 m thick at most, may be a block displaced from upslope, as are other small fragments of limestone, or may lie unconformably on the ophiolitic body, or may be in tectonic contact with it, but the block lacks a recovered underlying Miocene mudstone. However, various interpretations of recovered and nonrecovered contacts notwithstanding, it is clear that in the early Miocene an upslope instability caused movement of debris into either a canyon or another topographic low that allowed this debris to come to rest. Perhaps deep submarine erosion accompanied such a debris flow.

The lower part of the section was poorly recovered (less than 20%) and is composed of at least 135 m of tectonized ophiolitic material, including altered basalt, gabbro, diabase, serpentinitized peridotite (harzburgite), and serpentinite. The recovery of serpentinitized peridotite (harzburgite) at this site, at Site 566, and at two other localities by surface sampling from an oceanographic vessel (Ladd et al., 1978) indicates an extensive body of igneous rock in the lower slope. Despite the lack of datable material, it is clear that the igneous rock was tectonized prior to the early Miocene, because it is included in the early Miocene slope deposits covering the igneous rock. If the Cretaceous limestone was deposited as a sediment on the ophiolitic complex as it is on land in Costa Rica, the igneous rock is of the pre-late Campanian.

Benthic foraminiferal assemblages indicate water at or near present depth throughout the Neogene, with reworked fauna from upslope. Paleogene units upslope were identified in clasts including Oligocene mudstone and

middle Eocene diatomaceous mudstone probably deposited in abyssal environments. The Cretaceous limestone was deposited above the CCD, in contrast to the unit of equivalent age upslope in the Petrel Well deposited below the CCD.

Seismic velocity and density measurements of pieces of cored material reflect the variable lithologies drilled and show large pieces of rock probably had sealed the drill collars in the hole. Overpressure is consistent with the inferred subduction of trench sediment in which pore fluid pressures would respond to sudden loading by the overthrust block through which Hole 567A was being drilled. If the analysis of the seismic record is correct, the hole may have failed just 20 m from the top of the subducted sediment.

Geophysical and drilling data were used to develop structural interpretations of the base of the slope. These interpretations were discussed and diagrammed by several members of the scientific staff (Fig. 23) and the areas of agreement are very apparent. The base of the slope has no neogene accretionary prism, a conclusion also reached by the scientific staff of Leg 67. Collapse structure appears to dominate the first step of the margin above the subduction zone. The upper and lower plates appear highly decoupled across the subduction zone in order to accommodate extension in an environment of rapid convergence.

#### A Reexamination of Pre-Neogene Core from Leg 67, Hole 494A

Sites 494 and 567 are 110 m apart but were interpreted differently by the scientific staffs of Legs 67 and 84. The Leg 84 staff concluded that at Site 567 the lower part of the section contained redeposited lithologies that came

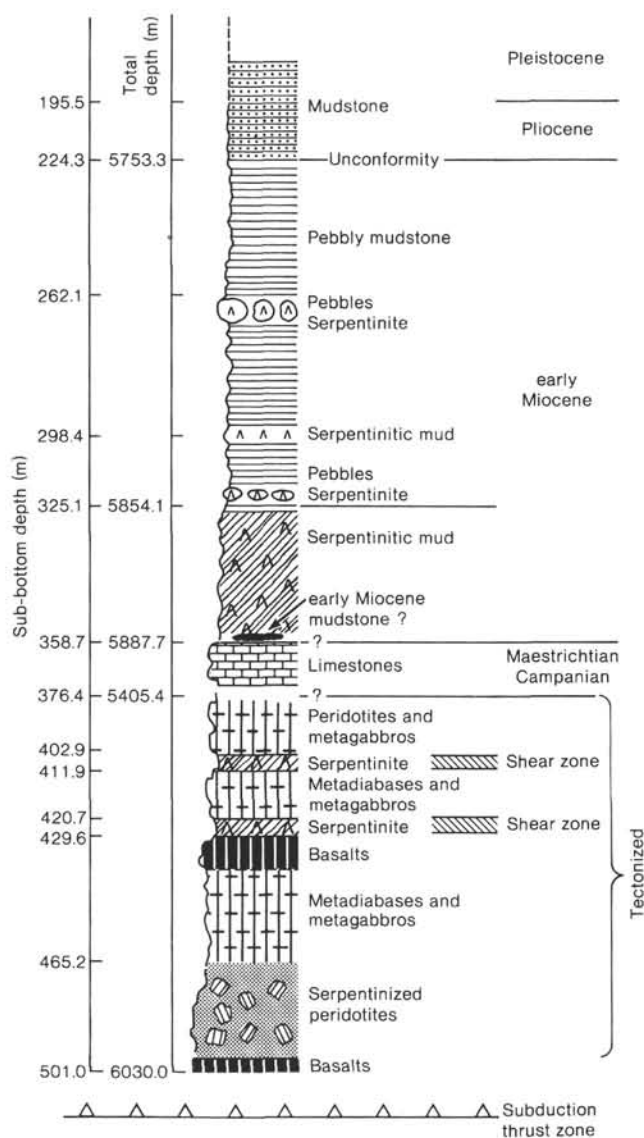


Figure 22. Summary of basal lithologies of Hole 567A.

from upslope during the Miocene, whereas the Leg 67 staff considered 53 m (between 294 and 241 m below the mudline) of a fractured, very dark gray mudstone as *in situ* middle Eocene. Thus a reexamination of Site 494 in light of the subsequent experience at Site 567 and other Leg 84 sites was made to see if the interpretations are more consistent than they seem at first glance.

The Site 494 core was highly fragmented and commonly consisted of angular drill cuttings. This condition began rather suddenly between Cores 494A-20 and -22. The fractured condition could have been caused by changes in drilling procedure, bit failure, or alternatively, it could have been from drilling of a highly fractured formation. The former interpretation was favored at the time of drilling, but when similar fragmentation was encountered at Hole 567, the latter interpretation seemed better.

The staffs of both legs noted that at Site 494 some fractured claystone sections are not completely disasso-

ciated but can be fit back together. Contacts, color bands, and beds can be traced across some cored intervals. Brecciation, well displayed in Core 27, is seen in fragments, particularly in more competent calcareous mudstones. Thus some of the rock was a breccia *in situ* or was fractured and then fragmented when drilled.

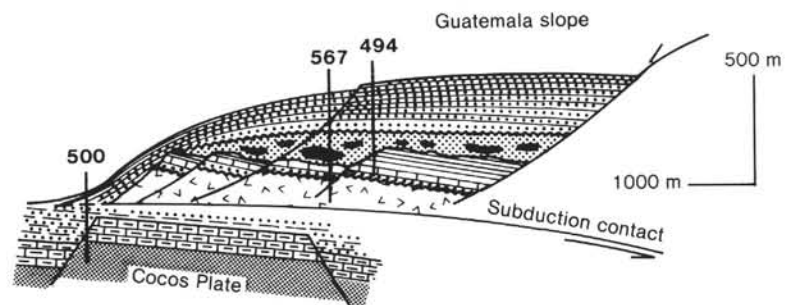
To test whether intervals where this relation is not so clear could also have consisted of fragmented rock rather than a mixture of lithologies from up the hole, fragments of different lithologies were examined paleontologically. The results of this and the Leg 67 studies are summarized in Figure 24. No displaced fauna or flora was found, and the results are in agreement with the Leg 67 conclusions. The normal ordering of fossil assemblages suggests little contamination, and the recovered material was probably from the interval cored.

With Leg 84 results in retrospect there is clear evidence of *in situ* redeposited debris from upslope in Core 494A-29 where many igneous pebbles from the ophiolitic basement were recovered. Thus it is unclear whether the underlying lithologies are transported or in place. Similarly, it is possible that the Cretaceous interval in Cores 494A-27 and -28, which is underlain by a middle Eocene interval, is a transported lithology. Thus if drilling contamination is considered minimal, the interpretations of sites 494 and 567 are generally consistent.

## REFERENCES

- Aubouin, J., Stephan, J. F., Renard, V., Roump, J., Lonsdale, P., 1981. Subduction of the Cocos Plate in the Middle America Trench. *Nature*, 294:146-150.
- Aubouin, J., von Huene, R., et al., 1982. *Init. Repts. DSDP*, 67: Washington (U.S. Govt. Printing Office).
- Barron, J.A., 1976. Revised Miocene and Pliocene diatom biostratigraphy of upper Newport Bay, Newport Beach, California. *Mar. Micropaleontol.*, 1:27-63.
- Bukry, D., 1971. Phytoplankton stratigraphy, central Pacific Ocean. In Winterer, E. L., Ewing, J. I., et al., *Init. Repts. DSDP*, 17: Washington (U.S. Govt. Printing Office), 871-890.
- Bukry, D., and Foster, J. H., 1971. Silicoflagellate and diatom stratigraphy, Leg 16, Deep Sea Drilling Project. In van Andel, Tj. H., Heath, G. R., et al., *Init. Repts. DSDP*, 16: Washington (U.S. Govt. Printing Office), 815-872.
- Burckle, L., 1972. Late Cenozoic planktonic diatom zones from the eastern equatorial Pacific. *First Symposium on Recent and Fossil Marine Diatoms, Nova Hedwigia*, 39:217-246.
- \_\_\_\_\_, 1977a. Pliocene and Pleistocene diatom datum levels from the equatorial Pacific. *Quat. Res.*, 7:330-340.
- \_\_\_\_\_, 1977b. Early Miocene to Pliocene diatom levels for the equatorial Pacific. Proceedings of the Second Working Group Meeting, Biostratigraphic Datum-Planes of the Pacific Neogene. IGCP Project 114. Republic of Indonesia, Ministry of Mines and Energy Spec. Publ. No. 1, pp. 25-44.
- Claypool, G. E., 1976. In Manual in Pollution Prevention and Safety, *JOIDES J.*, 1976/1(4):C7a.
- Gombos, A. M., Jr., 1975. Fossil diatoms for Leg 7, DSDP. *Micropaleontology*, 21(3).
- Gose, W. A., 1982. Some paleomagnetic results from DSDP Leg 67 off Guatemala. In Aubouin, J., von Huene, R., et al., *Init. Repts. DSDP*, 67: Washington (U.S. Govt. Printing Office), 669-674.
- Hesse, R., and Harrison, W. E., 1981. Gas hydrates (clathrates) causing pore-water freshening and oxygen isotope fractionation in deep water sedimentary sections of terrestrial continental margins. *Earth Planet. Sci. Lett.*, 55:453-462.
- Ibrahim, A. K., Latham, G. V., and Ladd, J. W., 1979. Seismic refraction and reflection measurements of the Middle America Trench offshore Guatemala. *J. Geophys. Res.*, 84:5643-5649.

- Joué, A. P., 1974. Diatoms in the Oligocene-Miocene biostratigraphic zones of the tropical areas of the Pacific Ocean. *Second Symposium on Recent and Fossil Diatoms*, Nova Hedwigia, 45.
- Kanaya, T., 1957. Eocene diatom assemblages from the Kellogg and Sidney shales, Mt. Diablo area, California. Tohoku Univ., Sendai, Japan.
- , 1971. Some aspects of pre-Quaternary diatoms in the oceans. In Funnell, B. M., and Riedel, W. R. (Eds.), *The Micropaleontology of Oceans*: New York (Cambridge University Press).
- Koezume, I., 1973. The late Cenozoic diatoms of Sites 183-193, Leg 19, DSDP. In Creager, J. S., Scholl, D. W., et al., *Init. Repts. DSDP*, 19: Washington (U.S. Govt. Printing Office), 805-856.
- Ladd, J. W., Ibrahim, A. K., McMillen, K. J., Latham, G. V., von Huene, R., 1982. Interpretation of seismic reflection data of the Middle America Trench offshore Guatemala. In Aubouin, J., von Huene, R., et al., *Init. Repts. DSDP*, 67: Washington (U.S. Govt. Printing Office), 675-690.
- Ladd, J. W., Ibrahim, A. K., McMillen, K. J., Latham, G. V., von Huene, R. E., Watkins, J. E., Moore, J. C., and Worzel, J. L., 1978. Tectonics of the Middle America Trench offshore Guatemala. *Init. Symp. of the Guatemala 4 Feb. Earthquake and Reconstruction Process*, Guatemala City, May 1978, Vol. 1.
- Moore, J. C., Biju-Duval, B. et al., in press. *Init. Repts. DSDP*, 78A: Washington (U.S. Govt. Printing Office).
- Moore, G. F., Lonsdale, P. F., and von Huene, R., 1982. Near bottom observations of the Middle America Trench off Guatemala. In Aubouin, J., von Huene, R., et al., *Init. Repts. DSDP*, 67: Washington (U.S. Govt. Printing Office), 707-718.
- Muhina, V. V., 1971. Problems of diatom silicoflagellate Quaternary stratigraphy in the equatorial Pacific Ocean. In Funnell, B. M., and Riedel, W. R. (Eds.), *The Micropaleontology of Oceans*: New York (Cambridge University Press).
- Muzylov, N., 1982. Nannoplankton stratigraphy of Leg 67 drill sites. In Aubouin, J., von Huene, R., et al., *Init. Repts. DSDP*, 67: Washington (U.S. Govt. Printing Office), 383-399.
- Schrader, H. J., 1974. Cenozoic marine planktonic diatom stratigraphy of the tropical Indian Ocean. In Fisher, R. L., Bunce, E. T., et al., *Init. Repts. DSDP*, 24: Washington (U.S. Govt. Printing Office), 887-967.
- , 1973. Cenozoic diatoms from the northeast Pacific, Leg 18. In Kulm, L. D., von Huene, R., et al., *Init. Repts. DSDP*, 18: Washington (U.S. Govt. Printing Office), 673-797.
- Seely, D., 1979. Geophysical investigations of continental slopes and rises. In Watkins, J. S., Montadert, L., and Dickerson, P. W. (Eds.), *Geologica and Geophysical Investigations of Continental Margins*: Tulsa, Oklahoma, Am. Assoc. Pet. Geol. Mem., 29: 245-260.
- Seely, D. R., Vail, P. R., and Walton, G. G., 1974. Trench-slope model. In Burke, C. A., and Drake, C. L. (Eds.), *The Geology of Continental Margins*: New York (Springer-Verlag), pp. 249-269.
- Sliter, W. V., 1968. Upper Cretaceous foraminifera from southern California and northwestern Baja California, Mexico. *Univ. of Kansas, Paleontologic Contrib.*, Serial No. 49, Article 7, 1-141.
- , 1977. Cretaceous foraminifers from the southwestern Atlantic Ocean, Leg 36, Deep Sea drilling Project. In Barker, P. F., Dalziel, I. W. D., et al., *Init. Repts. DSDP*, 36: Washington (U.S. Govt. Printing Office), 519-574.
- Thompson, P. R., 1982. Foraminifers of the Middle America Trench. In Aubouin, J., von Huene, R., et al., *Init. Repts. DSDP*, 67: Washington (U.S. Govt. Printing Office), 351-381.
- von Huene, R., Aubouin, J., et al., 1980. Leg 67: The Deep Sea Drilling Project Middle America Trench transect off Guatemala. *Geol. Soc. Am. Bull.*, 91(1):421-432.
- von Huene, R., Ladd, J., and Norton, I., 1982. Geophysical observations of slope deposits, Middle America Trench off Guatemala. In Aubouin, J., von Huene, R., et al., *Init. Repts. DSDP*, 67: Washington (U.S. Govt. Printing Office), 719-732.
- Watkins, J. S., Moore, J. C., et al., 1982. *Init. Repts. DSDP*, 66: Washington (U.S. Govt. Printing Office).
- Westberg, M. J., and Riedel, W. R., 1982. Radiolarians from the Middle America Trench off Guatemala, Deep Sea Drilling Project Leg 67. In Aubouin, J., von Huene, R., et al., *Init. Repts. DSDP*, 67: Washington (U.S. Govt. Printing Office), 401-424.
- Wornardt, W. W., 1967. Miocene and Pliocene marine diatoms from California. *Occasional Papers of the California Academy of Sciences*, San Francisco.



## Cocos Plate

Pleistocene  
Pliocene

Miocene (chalk)

Oceanic crust  
(basalt)

## Guatemala slope

Pleistocene

Pliocene

early Miocene  
(mafic mudstone)

Serpentinite

Eocene

Late Cretaceous  
(Campanian—Maestrichtian)

Ophiolite complex

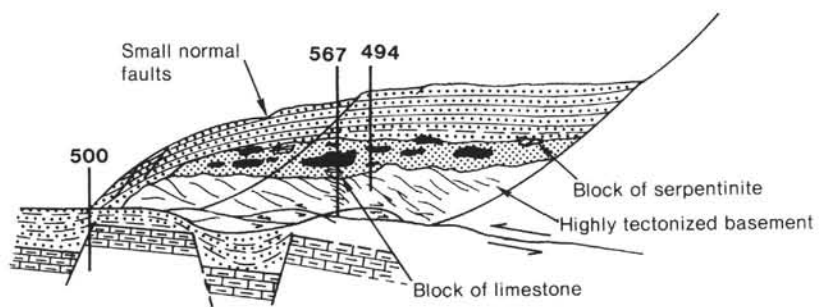
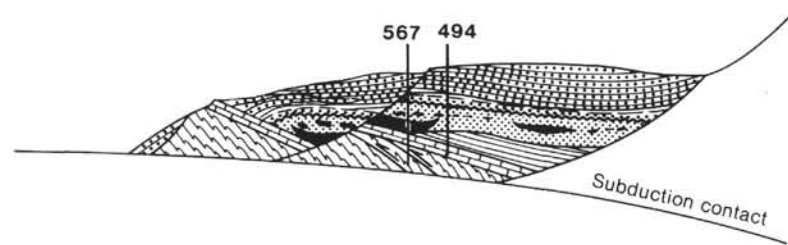


Figure 23. Proposed cross section of the Middle America Trench and slope and subducting plate off Guatemala.



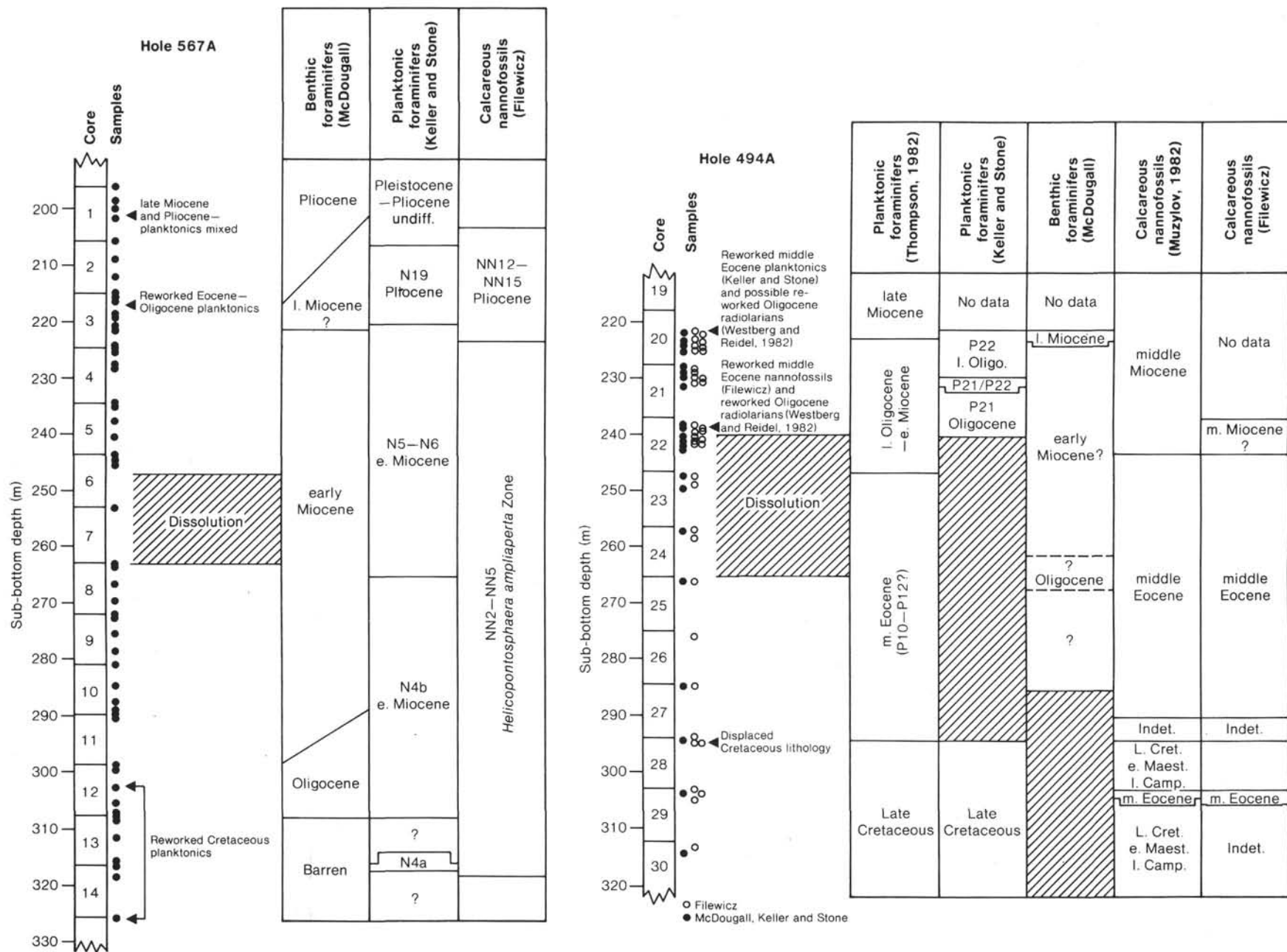


Figure 24. Results of paleontologic analysis of different lithologies recovered on Leg 67, Cores 494A-20 to -30, and comparison with Hole 567A of Leg 84.

SITE 567 HOLE		CORE H1		CORED INTERVAL 0.0–176.1 m sub-bottom						
TIME – ROCK UNIT	BIOSTRATIGRAPHIC ZONE	FOSSIL CHARACTER			SECTION METERS	GRAPHIC LITHOLOGY	DISTURBANCE SECONDARY STRUCTURES	SAMPLER SAMPLER SAMPLER	LITHOLOGIC DESCRIPTION	
		FORAMINIFERS	NANNOFOSSILS	RADIOLARIANS						DIATOMS
Pleistocene to middle Miocene					0.5				Shell fragment	Dominant lithology: diatomaceous mud. Color: dark olive gray (5Y 3/2). Structureless. Dispersed shelly fragments and sand sized grains. Mottling.
					1.0				Shell fragment	
					2				Shell fragment	Minor lithology: sand. Color: black (5Y 2.5/1). Massive, no internal structures.
					3					
					4					SMEAR SLIDE SUMMARY (%): 2, 140 3, 138 4, 140 6, 140 CC, 10 CC, 13
					5					
					6					Texture: Sand 5 5 80 15 16 10 Silt 15 15 5 25 84 30 Clay 80 80 5 60 – 60 Composition: Quartz 5 10 50 15 2 2 Feldspar 1 5 20 5 1 3 Mica – – – 2 1 Heavy minerals 2 2 5 2 1 1 Clay 67 50 7 37 – 90 Volcanic glass – Tr – 3 10 1 Glaucinite 3 3 10 2 – – Pyrite 3 – 5 3 – – Zeolite – – – Tr – – Carbonate unspc. – – – 3 84 – Foraminifers – – 3 – – – Calc. nannofossils Tr 1 – 25 – – Diatoms 10 20 Tr 3 – 1 Radiolarians 5 5 – 1 – 1 Sponge spicules 3 5 Tr 1 – 1 Silicoflagellates 2 – – – – –
					7					
					8					Grayish olive color (10Y 4/2)
					9					Light olive (10Y 5/4)
				10					Pale olive (10Y 6/2) mottling	
				11					Void	
				12					Void	
				13					Calcareous mudstone fragments. Veins of CaCO <sub>3</sub> cross-cut the mudstone. Shattered the rock. Carbonate bomb 69% CaCO <sub>3</sub> .	

SITE 567 HOLE		CORE 1		CORED INTERVAL 176.1–185.8 m sub-bottom	
TIME – ROCK UNIT	BIOSTRATIGRAPHIC ZONE	FOSSIL CHARACTER		SECTION METERS	GRAPHIC LITHOLOGY
		FORAMINIFERS	NANNOFOSSILS		
TIME – ROCK UNIT	BIOSTRATIGRAPHIC ZONE	FORAMINIFERS	NANNOFOSSILS	DIATOMS	LITHOLOGIC DESCRIPTION
		FORAMINIFERS	NANNOFOSSILS	DIATOMS	
early Pleistocene	Calicheal macrinyl				<p>Void</p> <p>Dominant lithology: diatomaceous mud. Color: dark olive gray (5Y 2.5/2). Highly deformed by drilling, no internal structures.</p>

SITE 567 HOLE		CORE 2		CORED INTERVAL 185.8–195.5 m sub-bottom	
TIME – ROCK UNIT	BIOSTRATIGRAPHIC ZONE	FOSSIL CHARACTER		SECTION METERS	GRAPHIC LITHOLOGY
		FORAMINIFERS	NANNOFOSSILS		
TIME – ROCK UNIT	BIOSTRATIGRAPHIC ZONE	FORAMINIFERS	NANNOFOSSILS	DIATOMS	LITHOLOGIC DESCRIPTION
		FORAMINIFERS	NANNOFOSSILS	DIATOMS	
early Pleistocene	Calicheal macrinyl				<p>Dominant lithology: mud. Color: dark olive gray (5Y 3/2). Some angular mudstone and sandstone clasts. Highly deformed by drilling disturbance.</p>

SITE	567	HOLE	A	CORE	H1	CORED INTERVAL	0.0–195.5 m sub-bottom
TIME – ROCK UNIT	BIOSTRATIGRAPHIC ZONE	FOSSIL CHARACTER	SECTION	METERS	GRAPHIC LITHOLOGY	DRILLING LOG DISTANCE STRUCTURE SAMPLES	LITHOLOGIC DESCRIPTION
				0.5			Dominant lithology: diatomaceous mud. Color: dark olive gray (5Y 4/1) to grayish olive (10Y 5/4). Some dispersed black grains and plagioclase and quartz grains dispersed.
				1			Minor lithology: sand. Color: moderate olive brown (5Y 4/4). Very small amount found within the Core Catcher.
				1.0			SMEAR SLIDE SUMMARY (%): 3, 145 CC, 10 CC, 13
							Texture: Sand 2 16 10 Silt 8 84 30 Clay 80 – 60 Composition: Quartz Tr 2 2 Feldspar 1 1 3 Mica – 2 1 Heavy minerals 1 1 – Clay 84 – 90 Volcanic glass – 10 1 Carbonate unsp. 84 – Diatoms 14 – 1 Radiolarians Tr – 1 Sponge spicules 5 – 1 Silicoflagellates Tr –
				2			
				3			
				4			
				CC			Bluish gray (5B 4/1) Mud clasts < 4 mm

SITE	567	HOLE	A	CORE	1	CORED INTERVAL	195.5–205.2 m sub-bottom
TIME – ROCK UNIT	BIOSTRATIGRAPHIC ZONE	FOSSIL CHARACTER	SECTION	METERS	GRAPHIC LITHOLOGY	DRILLING LOG DISTANCE STRUCTURE SAMPLES	LITHOLOGIC DESCRIPTION
				0.5			Light olive gray (5Y 5/2)
				1			Dominant lithology: siliceous mud. Color: dark olive gray (5Y 3/2). Mostly massive although some mottling is present.
				1.0			SMEAR SLIDE SUMMARY (%): 1, 20 1, 29 5, 137
							Texture: Sand 5 2 20 Silt 50 5 60 Clay 45 93 20 Composition: Quartz Tr 1 5 Feldspar 1 1 3 Mica Tr – – Heavy minerals – Tr Tr Clay 83 85 60 Volcanic glass – 1 – Glauconite Tr – – Carbonate unsp. 5 12 5 Diatoms – – 5 Radiolarians 1 – 2 Sponge spicules 10 – 5 Rock fragments – – 15
				2			
				3			
				4			Slightly sandier down core
				5			
				6			← Burrows Light gray (5Y 7/1)
				7			
				CC			← Sand grains

SITE 567		HOLE A		CORE 2		CORED INTERVAL		205.2-214.9 m sub-bottom	
TIME - ROCK UNIT	BIOSTRATIGRAPHIC ZONE	FOSSIL CHARACTER			SECTION METERS	GRAPHIC LITHOLOGY	DRILLING LOG	STRUCTURAL SAMPLES	LITHOLOGIC DESCRIPTION
		FORAMINIFERS	NAUFOSSILS	DIAZONES					
early Pliocene	<i>Ceratolites acutus</i> - <i>Ammolobos tricorniculatus</i>				0.5				Calcareous light olive brown mottle (5Y 5/6)
					1.0				
					2.0				Dominant lithology: siliceous mud. Color: dark grayish olive (5Y 3/2). Mostly structureless except for some white mottled areas. Sand content varies but never exceeds 30%.  Minor lithology: sand. Color: dark grayish olive (5Y 3/2). Lot of parallel alignment of grains and large angular grains of green mud. Some erosive bases.
					2.5				
					3.0				SMEAR SLIDE SUMMARY (%): 2, 110 3, 137 CC, 10  Texture: Sand: 15 5 10 Silt: 15 10 45 Clay: 70 85 45 Composition: Quartz: 10 3 3 Feldspar: 5 1 5 Mica: - - 1 Heavy minerals: 1 1 1 Clay: 55 80 72 Volcanic glass: Tr 1 15 Glauconite: 1 2 Tr Pyrite: 1 3 2 Carbonate unsp.: 1 2 - Foraminifera: - Tr - Calc. nanofossils: 10 1 - Diatoms: 10 1 1 Radiolarians: 5 1 - Sponge spicules: 1 3 2 Silicoflagellates: Tr - -
					3.5				
					4.0				Blue green rounded mud clasts Batal coarse sand
					4.5				
					5.0				Sandy mottling
					5.5				
					6.0				White clast
					6.5				
					7.0				
					CC				

SITE 567		HOLE A		CORE 3		CORED INTERVAL		214.9-224.6 m sub-bottom	
TIME - ROCK UNIT	BIOSTRATIGRAPHIC ZONE	FOSSIL CHARACTER			SECTION METERS	GRAPHIC LITHOLOGY	DRILLING LOG	STRUCTURAL SAMPLES	LITHOLOGIC DESCRIPTION
		FORAMINIFERS	NAUFOSSILS	DIAZONES					
early Pliocene	<i>Ceratolites acutus</i> - <i>Ammolobos tricorniculatus</i>				0.5				Dominant lithology: mud. Color: grayish olive green (5GY 3/2) to olive gray (5Y 3/2). Change takes place in Section 2 at 50 cm.
					1.0				
					2.0				Some fine laminations show up by the sandier parts of the section. A few erosion surfaces and graded beds. Some calcareous mottling.
					2.5				
					3.0				Fracturing of sediment is a result of drilling and early fracturing in the sedimentary pile.
					3.5				
					4.0				SMEAR SLIDE SUMMARY (%): 1, 105 1, 108 1, 130 3, 100  Texture: Sand: 5 2 5 40 Silt: 10 30 10 40 Clay: 85 68 85 20 Composition: Quartz: 4 1 3 10 Feldspar: 3 1 2 5 Mica: - 1 - 1 Heavy minerals: Tr Tr 2 1 Clay: 68 5 67 62 Volcanic glass: - 2 10 Palagonite: - 1 - Glauconite: 3 - 3 1 Pyrite: 5 - 5 - Carbonate unsp.: - 85 - 10 Calc. nanofossils: 2 - 1 - Diatoms: 1 1 1 - Radiolarians: 1 1 1 Tr Sponge spicules: - Tr 1 - Blue clay minerals: 3 - - -
					4.5				
					5.0				CARBONATE BOMB (% CaCO <sub>3</sub> ): 1, 108 cm = 17.5
					5.5				
					6.0				Pale olive clast Sandy layer - blue green (5BG 5/2) clasts
					6.5				
					7.0				Greenish gray (5GY 6/1) mottling
					7.5				
					CC				



SITE 567 HOLE A CORE 4 CORED INTERVAL 224.6–234.1 m sub-bottom

TIME – ROCK UNIT	BIOSTRATIGRAPHIC ZONE	FOSSIL CHARACTER			SECTION	METERS	GRAPHIC LITHOLOGY	DRILLING DISTURBANCE	SEDIMENTARY STRUCTURES	SAMPLES	LITHOLOGIC DESCRIPTION
		FORAMINIFERS	NANNOFOSSILS	RADIOLARIANS							
early Miocene	<i>Helicostaphira ampliparva</i>				1	0.5					<p>Dominant lithology: mud. Color: dark greenish gray (5GY 4/1). Very little internal structure. Between Section 3, 50–135 cm is a sedimentary breccia with mud clasts up to 2 cm in diameter. Some bioturbation.</p> <p>SMEAR SLIDE SUMMARY (%): 3, 100</p> <p>Texture: Sand 15 Silt 15 Clay 70</p> <p>Composition: Quartz 10 Feldspar 5 Clay 73 Volcanic glass Tr Palagonite Tr Glaucinite Tr Pyrite 3 Zeolite 1 Foraminifers Tr Calc. nannofossils 3 Diatoms 1 Radiolarians 1 Sponge spicules 3</p> <p>CARBONATE BOMB (% <math>\text{CaCO}_3</math>): 1, 70 cm = Tr</p> <p>CaCO<sub>3</sub> rich bioturbations</p> <p>Mottling</p> <p>Sedimentary breccia of angular mud clasts up to 1 cm in diameter</p>
					2	1.0					
					3						

SITE 567 HOLE A CORE 5 CORED INTERVAL 234.1–243.6 m sub-bottom

TIME – ROCK UNIT	BIOSTRATIGRAPHIC ZONE	FOSSIL CHARACTER			SECTION	METERS	GRAPHIC LITHOLOGY	DRILLING DISTURBANCE	SEDIMENTARY STRUCTURES	SAMPLES	LITHOLOGIC DESCRIPTION
		FORAMINIFERS	NANNOFOSSILS	RADIOLARIANS							
early Miocene	<i>Helicostaphira ampliparva</i>				1	0.5					<p>Sedimentary breccia – calcareous cement</p> <p>Dominant lithology: mudstone. Color: variable but pre-dominantly pale green (10G 6/2) to medium bluish gray (5B 5/1). Massive.</p> <p>Sedimentary breccia at the top of Section 1. Angular clasts up to 0.5 cm in diameter. Color clasts: yellowish gray (5Y 8/1) and light bluish gray (5B 7/1).</p> <p>Breccia is bioturbated as is mudstone.</p> <p>SMEAR SLIDE SUMMARY (%): 1, 90 2, 90</p> <p>Texture: Sand 5 5 Silt 10 15 Clay 85 80</p> <p>Composition: Quartz 3 5 Feldspar 2 2 Heavy minerals 1 Tr Clay 83 75 Volcanic glass 1 – Glaucinite – Tr Pyrite 2 3 Foraminifers Tr – Calc. nannofossils 3 5 Diatoms 1 2 Radiolarians 2 2 Sponge spicules 2 3</p> <p>Pale green (5G 7/2) mud</p> <p>Pale green (10G 6/2)</p> <p>Bluish gray (5B 5/1)</p> <p>Olive black mottling</p> <p>Calcareous mottling yellow (5Y 8/1)</p>
					2	1.0					
					3						

SITE 567		HOLE A		CORE 6		CORED INTERVAL 243.6–253.1 m sub-bottom	
TIME – ROCK UNIT	BIOSTRATIGRAPHIC ZONE	FOSSIL CHARACTER			SECTION METERS	GRAPHIC LITHOLOGY	LITHOLOGIC DESCRIPTION
		FORAMINIFERS	NANNOFOSSILS	RADIOLARIANS			
mixed early Miocene to Oligocene				R	0.5		Pebbles of dolomite and $\text{CaCO}_3$
					1		Dominant lithology: mudstone. Color: 0–460 cm dusky yellowish green (10GY 3/2). 460–660 cm variable – see below.
					1.0		Core is dominated by sedimentary breccias with angular clasts of mud up to 2 cm in diameter. Clasts vary in color: light blue (5B 7/6), grayish blue green (5BG 5/2), and pale yellowish green (10GY 7/2). Some <i>in situ</i> fracturing.
							Fractures
							Ash band 0.5 cm thick in Section 4.
					2		SMEAR SLIDE SUMMARY (%): 4, 84 4, 125
							Texture:
							Sand 5 75
							Silt 10 15
							Clay 85 10
					3		Composition:
							Quartz 5 50
							Feldspar 3 30
							Mica Tr –
							Heavy minerals Tr Tr
							Clay 76 10
							Volcanic glass 2 5
							Palagonite Tr –
							Pyrite 3 5
							Foraminifers 1 –
					4		Calc. nannofossils 3 Tr
							Diatoms 1 –
							Radiolarians 3 Tr
							Sponge spicules 3 –
							Carbonate rich above layer
							Sedimentary breccia – grayish blue green (5BG 5/2)
							Ash band
							Sedimentary breccia
							Sedimentary breccia
					5		

SITE 567		HOLE A		CORE 7		CORED INTERVAL 253.1–262.7 m sub-bottom	
TIME – ROCK UNIT	BIOSTRATIGRAPHIC ZONE	FOSSIL CHARACTER			SECTION METERS	GRAPHIC LITHOLOGY	LITHOLOGIC DESCRIPTION
		FORAMINIFERS	NANNOFOSSILS	RADIOLARIANS			
early Miocene	<i>Helicospira amplogerta</i>				0.5		Dominant lithology: mudstone. Color: grayish olive green (5GY 3/2) to pale green (10G 6/2).
					1		Structureless – dominated by sedimentary breccias with blue clast up to 2 cm in diameter. Matrix and clast supported. Dolomitic around serpentine clasts.
					1.0		Minor lithology: serpentine. Color: dusky blue (5PB 3/2) to grayish blue (5PB 5/2). Present as large clasts within the mud. Original structures visible – truncated at margins of the boulder. Larger boulder may comprise smaller clasts.
							SMEAR SLIDE SUMMARY (%): 1, 15 2, 139 2, 145
							Texture:
							Sand 10 6 –
							Silt 15 70 –
							Clay 75 24 –
							Composition:
							Quartz 12 2 –
					2		Feldspar 4 1 –
							Mica 1 – –
							Heavy minerals 1 – 2
							Clay 70 72 –
							Volcanic glass 5 5 –
							Pyrite – – 3
							Sponge spicules 1 – –
							Serpentine 80 – –
							Dolomite 15 – 20
							CARBONATE BOMB (% $\text{CaCO}_3$ ): 2, 139 cm = 21

SITE 567		HOLE A		CORE 8		CORED INTERVAL		262.7–271.9 m sub-bottom	
TIME – ROCK UNIT	BIOSTRATIGRAPHIC ZONE	FOSSIL CHARACTER			SECTION	METERS	GRAPHIC LITHOLOGY	DRILLING DISTURBANCE STRUCTURES	LITHOLOGIC DESCRIPTION
		FORAMIFERS	NANNOFOSSILS	RADIOLARIANS					
early Miocene	<i>S. belemnus-H. anguligera</i>	R	R		1	0.5	Void		Dominant lithology: mudstone. Color: dusky green (5G 3/2) to olive gray (5Y 3/2).
						1.0	Void		
					2				Full of sedimentary breccias with assorted clasts up to 1 cm in diameter. Color of clasts: pale blue (5PB 7/2), light blue (5B 7/6), and grayish yellow (5Y 8/4).
					3				Some bioturbation – usually calcareous.
					4				SMEAR SLIDE SUMMARY (%): 1, 140, 3, 126
					5				Texture: Sand 5 6 Silt 20 56 Clay 75 38 Composition: Quartz 2 1 Feldspar 1 – Heavy minerals Tr 2 Clay 87 35 Volcanic glass – 5 Pyrite 1 – Carbonate unsp. 5 50 Diatoms 1 Tr Radiolarians 2 Tr Sponge spicules 1 1 Fecal pellets – 4
					6				CARBONATE BOMB (% CaCO <sub>3</sub> ): 3, 129 cm = 50
					CC				Dominant lithology: mudstone. Color: grayish olive (10Y 4/2). Lots of drilling deformation so little or no structures seen. Some bioturbation and ash bands seen in Section 5.

SITE 567		HOLE A		CORE 9		CORED INTERVAL		271.9–280.7 m sub-bottom	
TIME – ROCK UNIT	BIOSTRATIGRAPHIC ZONE	FOSSIL CHARACTER			SECTION	METERS	GRAPHIC LITHOLOGY	DRILLING DISTURBANCE STRUCTURES	LITHOLOGIC DESCRIPTION
		FORAMIFERS	NANNOFOSSILS	RADIOLARIANS					
early Miocene	<i>S. belemnus-H. anguligera</i>				1	0.5			Pyrite rich nodule Ash band pale red purple (5RP 6/2)
						1.0			
					2				Bioturbation
					3				SMEAR SLIDE SUMMARY (%): 1, 61 3, 46 5, 131 CC, 10
					4				Texture: Sand 80 15 10 6 Silt 15 75 15 50 Clay 5 10 75 44 Composition: Quartz 2 2 10 1 Feldspar 5 3 55 1 Clay 1 77 – 80 Volcanic glass 88 – 30 – Palagonite Tr – – Glaucinite – Tr – Tr Pyrite 2 5 3 4 Carbonate unsp. 2 10 2 10 Foraminifers – Tr – Tr Calc. nanofossils – Tr – – Diatoms Tr Tr – 1 Radiolarians – 1 Tr 1 Sponge spicules – 2 Tr Tr Silicoflagellates – – Tr –
					5				CARBONATE BOMB (% CaCO <sub>3</sub> ): 10%
					6				Pyrite Black mottling Some ash bands – medium light gray (N6)
					CC				

SITE	567	HOLE A	CORE 10	CORED INTERVAL	280.7–289.5 m sub-bottom
TIME – ROCK UNIT	BIOSTRATIGRAPHIC ZONE	FOSSIL CHARACTER	SECTION METERS	GRAPHIC LITHOLOGY	LITHOLOGIC DESCRIPTION
	FORAMINIFERS	NANNOFOSSILS	RADIOLARIANS	DIAZONES	
early Miocene <i>S. inferius-H. anguligera</i>					Void
					0.5
					1
					1.0
					2
					3
					4
					5
					6
					7
				CC	Void

Dominant lithology: mudstone. Color: grayish olive green.  
Structureless – due to drilling deformation.

Minor lithology: conglomerate. Color: generally grayish green (5G 5/2). Mostly rounded clasts up to 5 cm in diameter. Limestones, andesite and green mud pebbles. Mudstone matrix. Possibility this is drilling – not likely in context of rest of this unit.

SMEAR SLIDE SUMMARY (%):  
1, 63 2, 134

Texture:

Sand	20	4
Silt	70	46
Clay	10	50

Composition:

Quartz	2	1
Feldspar	3	1
Mica	Tr	—
Heavy minerals	1	Tr
Clay	63	88
Volcanic glass	15	—
Glaucinite	—	Tr
Pyrite	1	—
Carbonate unspc.	—	10
Foraminifera	1	—
Diatoms	1	—
Radiolarians	1	—
Sponge spicules	2	—

CARBONATE BOMB (% CaCO<sub>3</sub>):  
2, 134 cm = 10

Dispersed glassy tuff dark green mottling

Conglomerate

Greenish gray (5G 5/1) clasts

SITE	567	HOLE	A	CORE	11	CORED INTERVAL	289.5-298.4 m sub-bottom
TIME - ROCK UNIT	BIOSTRATIGRAPHIC ZONE	FOSSIL CHARACTER	SECTION	METERS	GRAPHIC LITHOLOGY	DRELLING DISTURBANCE STRUCTURES	LITHOLOGIC DESCRIPTION
		FORAMINIFERS NANNOFOSSELS RADIOLARIANS DIATOMS				SAMPLES	
early Miocene and Oligocene mixed				0.5			
			1	1.0		*	*  Light gray limestone clasts  Dominant lithology: siliceous mudstone. Color: dark greenish gray (SG 4/1) at top grading down to greenish gray (SG 5/1).  Structureless. Some dispersed sand sized particles - "gritty texture". Some clasts of limestone present.  Minor lithology: limestone. Color: light gray (N7). Present as clasts in mudstone. Veins of calcite all the way through. Similar to clasts in conglomerate of Core 10.
			2			*	*  SMEAR SLIDE SUMMARY (%): 1, 100  Texture: Sand 4 Silt 50 Clay 46  Composition: Quartz 1 Feldspar 1 Heavy minerals Tr Clay 63 Glauconite - Pyrite 2 Carbonate unspc. 20 Calc. nannofossils 1 Diatoms Tr Radiolarians 2 Sponge spicules 10 Silicoflagellates Tr  CARBONATE BOMB (% CaCO <sub>3</sub> ): 1, 80 cm = 20 2, 80 cm = 10



SITE 567 HOLE A CORE 12 CORED INTERVAL 298.4–307.3 m sub-bottom

TIME – ROCK UNIT	BIOSTRATIGRAPHIC ZONE	FOSSIL CHARACTER				SECTION METERS	GRAPHIC LITHOLOGY	DISTURBANCE STRUCTURES	SAMPLES	LITHOLOGIC DESCRIPTION
		FORAMINIFERS	NANNOFOSSILS	RADIOLARIANS	DIATOMS					
early Miocene	<i>Helicospira ampliperta</i>					0.5				Dominant lithology: mud. Color: dark greenish gray (5GY 4/1).
						1				
						1.0				Sedimentary breccia
										Slightly darker dark greenish gray (5G 4/1)
										SMEAR SLIDE SUMMARY (%): 2, 82 4, 12 5, 66 5, 84
										Texture:
										Sand 5 5 5 5
										Silt 15 15 30 15
										Clay 80 80 85 80
										Composition:
										Quartz 2 2 Tr 3
										Feldspar Tr Tr Tr Tr
										Mica – Tr –
										Heavy minerals Tr Tr Tr Tr
										Clay – – 10 70
										Volcanic glass 1 1 Tr 1
										Glauconite – – 3
										Pyrite – Tr 3
										Carbonate unsp. 3 100 1
										Foraminifers 1 – –
										Calc. nannofossils 5 Tr 5
										Diatoms 1 – Tr
										Radiolarians 1 – 1
										Sponge spicules – – 2
										CARBONATE BOMB (% CaCO <sub>3</sub> ): 4, 15 cm = 70
										Rounded clasts of blue green mudstone and olive green mud
										Clast of nanno ooze (light greenish gray)
										Clast of nanno ooze 5B 7/1

SITE 567 HOLE A CORE 13 CORED INTERVAL 307.3–316.2 m sub-bottom

TIME – ROCK UNIT	BIOSTRATIGRAPHIC ZONE	FOSSIL CHARACTER				SECTION METERS	GRAPHIC LITHOLOGY	DISTURBANCE STRUCTURES	SAMPLES	LITHOLOGIC DESCRIPTION
		FORAMINIFERS	NANNOFOSSILS	RADIOLARIANS	DIATOMS					
early Miocene	<i>Helicospira ampliperta</i>					0.5				Dominant lithology: mudstone. Color: greenish gray (5G 6/1) to grayish green (5G 5/2).
						1				
						1.0				Generally structureless except for a few laminations in Section 1. Lots of clasts of mudstone, very dark grayish brown (2.5Y 3/2) and very dark olive gray (5Y 3/2). Limestone and sandstone clasts as well.
										SMEAR SLIDE SUMMARY (%): 1, 90 1, 148 2, 17
										Texture:
										Sand 5 0 3
										Silt 10 20 7
										Clay 85 80 90
										Composition:
										Quartz 10 – 1
										Feldspar 3 – Tr
										Heavy minerals 1 – Tr
										Clay – 70 –
										Volcanic glass 1 – 1
										Glauconite – Tr 5
										Pyrite 3 Tr 3
										Carbonate unsp. 3 100 1
										Foraminifers 1 – –
										Calc. nannofossils 5 Tr 5
										Diatoms 1 – Tr
										Radiolarians 1 – 1
										Sponge spicules 1 – Tr
										CARBONATE BOMB (% CaCO <sub>3</sub> ): 1, 15 cm = 10
										Sedimentary breccia
										Some bioturbation and laminations
										Medium gray mud with bluish gray limestone clasts
										Sandstone clast
										Void
										CC

SITE 567 HOLE A CORE 14 CORED INTERVAL 316.2–325.1 m sub-bottom

TIME – ROCK UNIT	BIOSTRATIGRAPHIC ZONE	FOSSIL CHARACTER				SECTION METERS	GRAPHIC LITHOLOGY	DISTURBANCE STRUCTURES	SAMPLES	LITHOLOGIC DESCRIPTION
		FORAMINIFERS	NANNOFOSSILS	RADIOLARIANS	DIATOMS					
						0.5				Sedimentary breccia
						1				
						1.0				Dominant lithology: mud. Color: brownish black (5YR 2/1) to olive black (5Y 2/1). Massive mudstone – sedimentary breccia with assorted clasts.
										Minor lithology: serpentinite. Color: very pale blue (5B 8/2) and black – unweathered.
										SMEAR SLIDE SUMMARY (%): 2, 122
										Composition:
										Serpentinite 100
										Site 567A, Core 15, 325.1–334.0 m sub-bottom: no recovery.
										Sedimentary breccia
										Serpentinite clasts
										Yellowish gray limestone
										Weathered serpentinite
										Serpentinite
										Serpentinite clast
										CC

SITE 567 HOLE A CORE 16 CORED INTERVAL 334.0–342.8 m sub-bottom


TIME – ROCK UNIT	BIOSTRATIGRAPHIC ZONE	FOSSIL CHARACTER			SECTION METERS	GRAPHIC LITHOLOGY	DRILLING DISTURBANCE SEDIMENTARY STRUCTURES EXPOSURE SAMPLES	LITHOLOGIC DESCRIPTION
		FORAMINIFERS	NANNOFOSSILS	RADIOLARIANS				
					0.5 1 1.0 2 CC			<p>Dominant lithology: serpentinite. Color: pale blue green (5BG 7/2) mottled with pale blue (5PB 7/2).</p> <p>Highly deformed by drilling but some deformation is possibly original, i.e., due to shearing.</p> <p>Only one sample of unshered rock in Section 1, 20–30 cm. Lower down in the core black (5G 2/1) phacoids of serpentinite surrounded by weathered serpentinite.</p>

SITE 567 HOLE A CORE 17 CORED INTERVAL 342.8–351.7 m sub-bottom

TIME – ROCK UNIT	BIOSTRATIGRAPHIC ZONE	FOSSIL CHARACTER			SECTION METERS	GRAPHIC LITHOLOGY	DRILLING DISTURBANCE SEDIMENTARY STRUCTURES EXPOSURE SAMPLES	LITHOLOGIC DESCRIPTION
		FORAMINIFERS	NANNOFOSSILS	RADIOLARIANS				
					0.5 1 1.0 2 3 CC			<p>Dominant lithology: serpentinite. Color: dusky green (5G 3/2) and dusky blue (5PB 3/2) to black (N5).</p> <p>Weathered to a clayey texture. Deformed by drilling.</p> <p>Breccia of serpentinite</p> <p>Black mud with pyrite and volcanic glass</p> <p>Yellow pebbles of mudstone</p> <p>Very dark to black (N5) serpentinite. Weathered to clayey texture. Volcanic glass mixed in.</p> <p>Void</p> <p>SMEAR SLIDE SUMMARY (%):</p> <p>1, 80</p> <p>Texture:</p> <p>Sand 30</p> <p>Silt 10</p> <p>Clay 60</p> <p>Composition:</p> <p>Clay (serpentinite) 50</p> <p>Volcanic glass 30</p> <p>Pyrite 20</p>

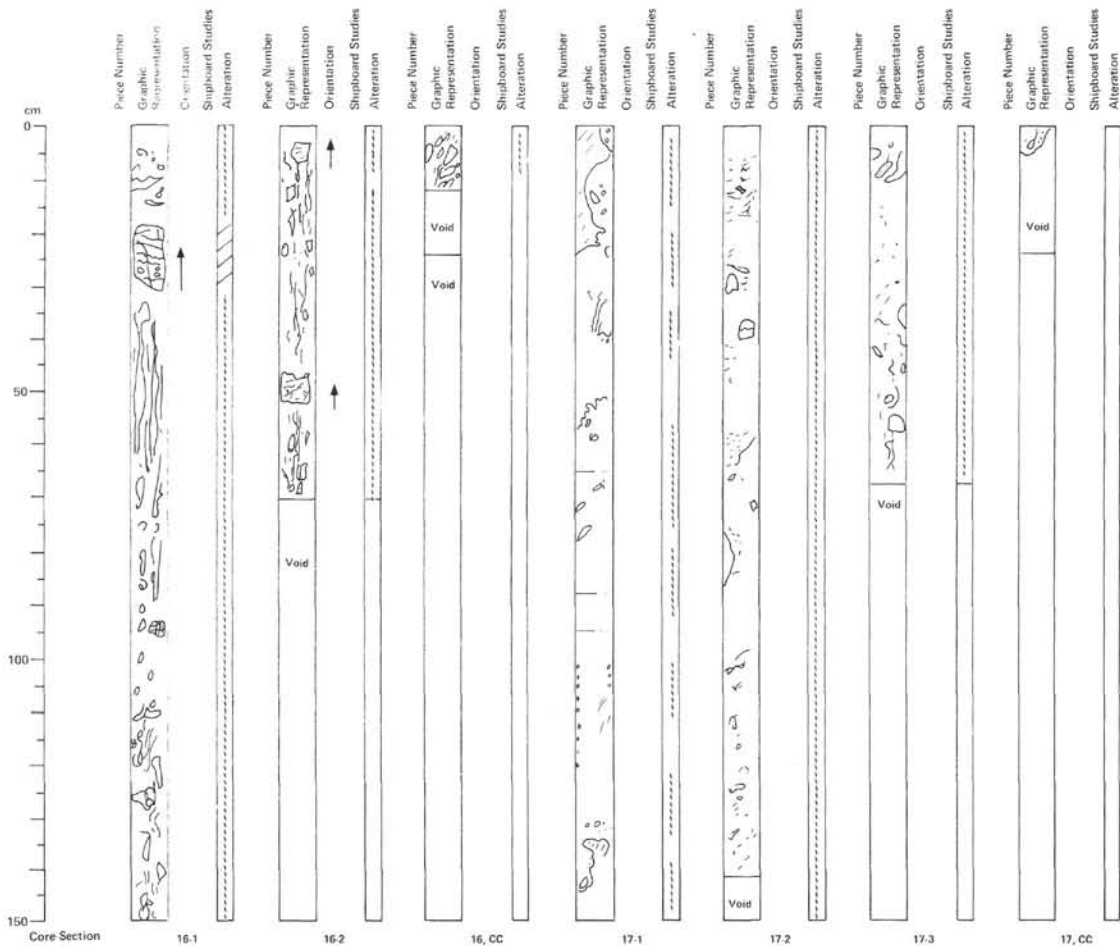
SITE 567 HOLE A CORE 18 CORED INTERVAL 351.7–358.7 m sub-bottom

TIME – ROCK UNIT	BIOSTRATIGRAPHIC ZONE	FOSSIL CHARACTER			SECTION METERS	GRAPHIC LITHOLOGY	DRILLING DISTURBANCE SEDIMENTARY STRUCTURES EXPOSURE SAMPLES	LITHOLOGIC DESCRIPTION
		FORAMINIFERS	NANNOFOSSILS	RADIOLARIANS				
early Miocene–Eocene mixed					0.5 1 1.0 CC			<p>Drilling breccia</p> <p>Altered clast of pale blue (5B 6/2) serpentinite</p> <p>Mixed lithologies</p> <p>Dominant lithology: drilling breccia comprising angular to sub-rounded clasts of:</p> <p>1) Mudstone. Color: medium dark gray (N4/5).</p> <p>2) Mudstone. Color: pale blue green (5BG 7/2).</p> <p>3) Altered serpentinite. Color: pale blue (5B 6/2).</p> <p>4) Sandstone. Color: brownish black.</p> <p>5) Light gray (N8) nanno ooze.</p> <p>SMEAR SLIDE SUMMARY (%):</p> <p>CC, 5–6</p> <p>Texture:</p> <p>Sand Tr</p> <p>Silt Tr</p> <p>Clay –</p> <p>Composition:</p> <p>Carbonate unspc. 80</p> <p>Calc. nannofossils 20</p>

SITE 567		HOLE A		CORE 19		CORED INTERVAL		358.7–368.4 m sub-bottom	
TIME – ROCK UNIT	BIOSTRATIGRAPHIC ZONE	FOSSIL CHARACTER			SECTION METERS	GRAPHIC LITHOLOGY	DRILLING DISTURBANCE SEDIMENTARY STRUCTURES	SAMPLES	LITHOLOGIC DESCRIPTION
		FORAMINIFERS	NANNOFOSSILS	RADIOLARIANS					
Cretaceous (Campanian–Maastrichtian)	A				0.5				<p>Drilling breccia limestone cuttings</p> <p>Dominant lithology: limestone. Color: pale red (10R 6/2) to pale greenish yellow (10Y 8/2).</p> <p>Pale red (10R 6/2) mottled limestone</p> <p>Mottled limestone. Fractured throughout. Some bedding visible.</p> <p>Pale green (10G 6/2) mottled limestone – well bedded</p> <p>Minor lithology: dolerite. Color: grayish green (10G 4/2).</p> <p>Pale greenish yellow (10Y 8/2) to very pale orange (10YR 8/2) mottled limestone</p> <p>Igneous rock</p> <p>SMEAR SLIDE SUMMARY (%): 1, 7</p> <p>Texture: Sand 30 Silt 50 Clay 20</p> <p>Composition: Quartz 10 Feldspar 5 Mica 1 Heavy minerals 2 Clay 10 Volcanic glass 3 Glauconite 1 Pyrite 3 Carbonate unsp. 52 Calc. nannofossils 5 Diatoms 1 Radiolarians 1 Sponge spicules 1 Serpentine 3</p> <p>CARBONATE BOMB (% <math>\text{CaCO}_3</math>): 1, 8 cm = 25 1, 85 cm = 58</p> <p>Section 1, 70 cm: fractures</p> 
					1.0				


SITE 567		HOLE A		CORE 20		CORED INTERVAL		368.4–386.1 m sub-bottom	
TIME – ROCK UNIT	BIOSTRATIGRAPHIC ZONE	FOSSIL CHARACTER			SECTION METERS	GRAPHIC LITHOLOGY	DRILLING DISTURBANCE SEDIMENTARY STRUCTURES	SAMPLES	LITHOLOGIC DESCRIPTION
		FORAMINIFERS	NANNOFOSSILS	RADIOLARIANS					
					0.5				<p>Drilling breccia</p> <p>Dominant lithology: gabbro and diabase – possibly clasts in a conglomerate. No matrix seen but could be to blue green mud. Alternative is that it is basement?</p> <p>Light green (5G 6/6) mud</p> <p>Gabbro</p> <p>Diabase</p> <p>Gabbro</p> <p>Drilling breccia: 1) Olive gray (5Y 3/2) mud. 2) Serpentine. 3) Grayish green (10GY 4/4) limestone. 4) Black (N1) peridotite.</p> <p>SMEAR SLIDE SUMMARY (%): 1, 20</p> <p>Texture: Sand 30 Silt 30 Clay 40</p> <p>Composition: Quartz 15 Feldspar 5 Heavy minerals Tr Clay 40 Volcanic glass Tr Glauconite 5 Pyrite 3 Carbonate unsp. 1 Serpentine 30</p>
					1.0				

SITE 567		HOLE A		CORE 21		CORED INTERVAL		386.1–402.9 m sub-bottom	
TIME – ROCK UNIT	BIOSTRATIGRAPHIC ZONE	FOSSIL CHARACTER			SECTION METERS	GRAPHIC LITHOLOGY	DRILLING DISTURBANCE SEDIMENTARY STRUCTURES	SAMPLES	LITHOLOGIC DESCRIPTION
		FORAMINIFERS	NANNOFOSSILS	RADIOLARIANS					
					CC				<p>Dominant lithology: igneous rock – see visual core description sheet.</p> <p>Three main rock types found within the Core Catcher: i) Microgabbro (dark yellowish green – 10GY 4/4). ii) Gabbro (grayish green – 10GY 5/2). iii) Dolerite (dusky green – 5G 3/2).</p>





84-567A-16-1	Depth 334.0–335.5 m
0–18 cm and 30–150 cm: serpentinite mud and drilling breccia, pale blue green (5BG 7/2) with pale blue (5PB 7/2) and dusky green (5G 3/2) streaks and pieces of more solid serpentinite up to 3 cm diameter.	
18–30 cm: massive black serpentinite with <10% pyroxene (harzburgite).	
84-567A-16-2	Depth 335.5–336.2 m
0–77 cm: serpentinite mud and drilling breccia, pale blue green (5BG 7/2) with streaks of pale blue (5PB 7/2), dusky green (5G 3/2) and greenish black (5G 2/1). More solid pieces of massive black serpentinite are surrounded by darker mud/drill breccia (greenish black – 5G 2/1).	
84-567A-16, CC	Depth 342.7–342.8 m
0–14 cm: serpentinite mud/drill breccia containing angular pieces up to 5 cm across of more solid serpentinite and white crystalline aggregate (calc?).	
84-567A-17-1	Depth 342.8–351.7 m
0–56 cm: serpentinite mud and drill breccia, medium bluish gray (5B 5/1) with streaks of grayish black (5GY 2/1) and small (<1 cm) pieces of more solid serpentinite.	
56–104 cm: black serpentinite mud containing pyrite.	
145–150 cm: volcanic ash, chlorite and small pieces of more solid serpentinite.	
104–145 cm: as in interval immediately above, except this later also contains small rounded pieces of serpentinite and yellowish mudstone(?) along the core liner. These are probably a drilling artifact.	
84-567A-17-2	Depth 351.7–353.1 m
0–65 cm: very dark serpentinitic mud/drill breccia with volcanic glass and pyrite admixture.	
65–140 cm: serpentinite mud/drill breccia (dusky blue – 5PB 3/2) with pieces of hard massive serpentinite or unbrecciated serpentinite breccia (greenish black – 5G 2/1).	
84-567A-17-3	Depth 353.1–353.8 m
Serpentinite mud/drill breccia, dusky green (5G 3/2) to dusky blue (5PB 3/2). White carbonate veins or brecciated veins.	
84-567A-17, CC	Depth 353.8–353.9 m
0–5 cm: as in Section 3.	

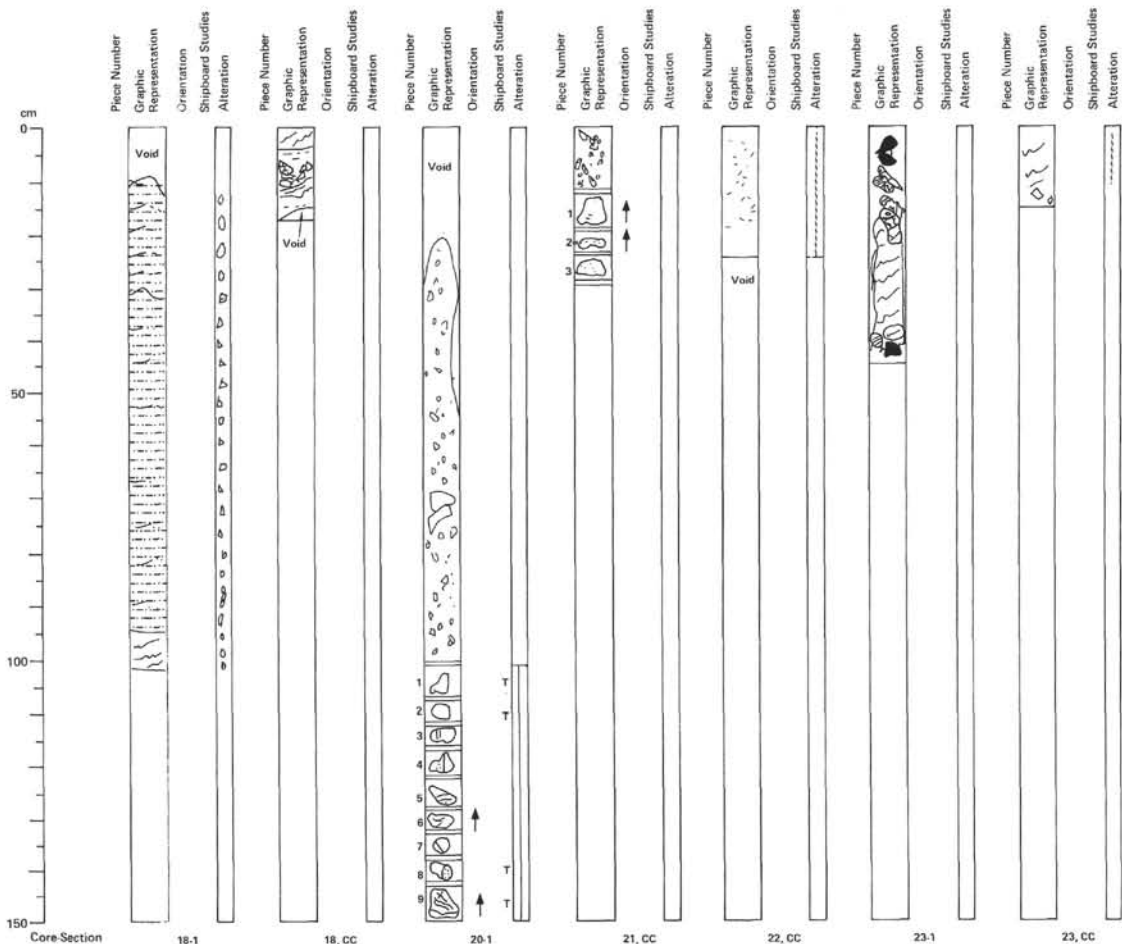
SITE 567 HOLE A CORE 22 CORED INTERVAL 402.9–411.8 m sub-bottom

TIME - ROCK UNIT	BIOSTRATIGRAPHIC ZONE	FOSSIL CHARACTER			SECTION	METERS	GRAPHIC LITHOLOGY	DRILLING REMARKS	SECONDARY STRUCTURES	SAMPLES	LITHOLOGIC DESCRIPTION
		FORAMINIFERS	NANNOFOSSILS	RADIOLARIANS							
					CC						Dominant lithology: serpentinite. Color: grayish blue (SPB 5/6).  Weathered/crusted to a mud. Several original pieces remain.  > 90% serpentinite.

SITE 567 HOLE A CORE 23 CORED INTERVAL 411.8–420.7 m sub-bottom

TIME - ROCK UNIT	BIOSTRATIGRAPHIC ZONE	FOSSIL CHARACTER			SECTION	METERS	GRAPHIC LITHOLOGY	DRILLING REMARKS	SECONDARY STRUCTURES	SAMPLES	LITHOLOGIC DESCRIPTION
		FORAMINIFERS	NANNOFOSSILS	RADIOLARIANS							
					1						Dominant lithology: igneous rock. i) Serpentinite mud (bluish gray - SB 8/11. ii) Diabase. iii) Gabbro.
					CC 0.5						<p>SMEAR SLIDE SUMMARY (%):</p> <p>1, 10</p> <p>Texture:</p> <p>Sand 60</p> <p>Silt 30</p> <p>Clay 10</p> <p>Composition:</p> <p>Talc 70</p> <p>Serpentine 30</p>





0–10 cm: void.

94-101 cm: blue green (5BG 6/2) serpentinite mud with carbonate veins and small pieces of harder serpentinite.

Highly varied, controversial sample.

0-4 and 10-13 cm: blue green serpentinite mud.

4-6 and 13-16 cm: olive gray mud.

6-10 cm: angular clasts of brownish black (5YR 4/1) silty sandstone, very light gray (N8) nanno oolite, and brown sandstone. Olive gray mud is Miocene in age, other clasts contain Eocene and Cretaceous microfossils.

25–100 cm: drill breccia of diabase and basalt.

0-10 cm: meta-gabbro drill breccia.

Pieces 1 and 2: meta-gabbro metamorphosed to greenschist facies.

Piece 3: meta-diorite metamorphosed to greenschist facies.

84-567A-22, CC Depth: 441.6–441.8 m  
0–24 cm: serpentinite mud/drill breccia, grayish blue (5PB 5/6) with more solid pieces of serpentinite <1.5 cm diameter.

84-567A-23 | Depth 411.8–420.7 m

0–44 cm: mixture of bluish gray (5B 5/1) serpentinite mud containing pieces of meta-diorite, meta-gabbro, and solid, annealed serpentinite breccia from sand-sized to 4 cm diameter. Massive serpentinite breccia contains pyrite crystals and veins of a soft white mineral (talc?).

0–12 cm: bluish gray (5B 6/1) serpentinite mud containing coarse sand-sized clasts of meta-diorite (black — N9).

SITE 567 HOLE A CORE 24 CORED INTERVAL 420.7–429.6 m sub-bottom

TIME – ROCK UNIT	BIOSTRATIGRAPHIC ZONE	FOSSIL CHARACTER			SECTION METERS	GRAPHIC LITHOLOGY	DRILLING DISTURBANCE STRUCTURES	SAMPLES	LITHOLOGIC DESCRIPTION
		FORAMINIFERS	NANNOFOSSILS	RADIOLARIANS					
					0.5 1 1.0 CC				Dominant lithology: serpentinite mud. Color: grayish blue (5PB 8/2) to pale blue (5PB 7/2).  Weathered to a mud.

SITE 567 HOLE A CORE 25 CORED INTERVAL 429.6–438.5 m sub-bottom

TIME – ROCK UNIT	BIOSTRATIGRAPHIC ZONE	FOSSIL CHARACTER			SECTION METERS	GRAPHIC LITHOLOGY	DRILLING DISTURBANCE STRUCTURES	SAMPLES	LITHOLOGIC DESCRIPTION
		FORAMINIFERS	NANNOFOSSILS	RADIOLARIANS					
					0.5 1 1.0 2 3				Dominant lithology: igneous rock. i) Gabbro. ii) Basalt – sheared, unshaped, and bedded. Possible pillowed margin.  All are metamorphosed.  See igneous rock sheet.

SITE 567 HOLE A CORE 26 CORED INTERVAL 438.5–445.8 m sub-bottom

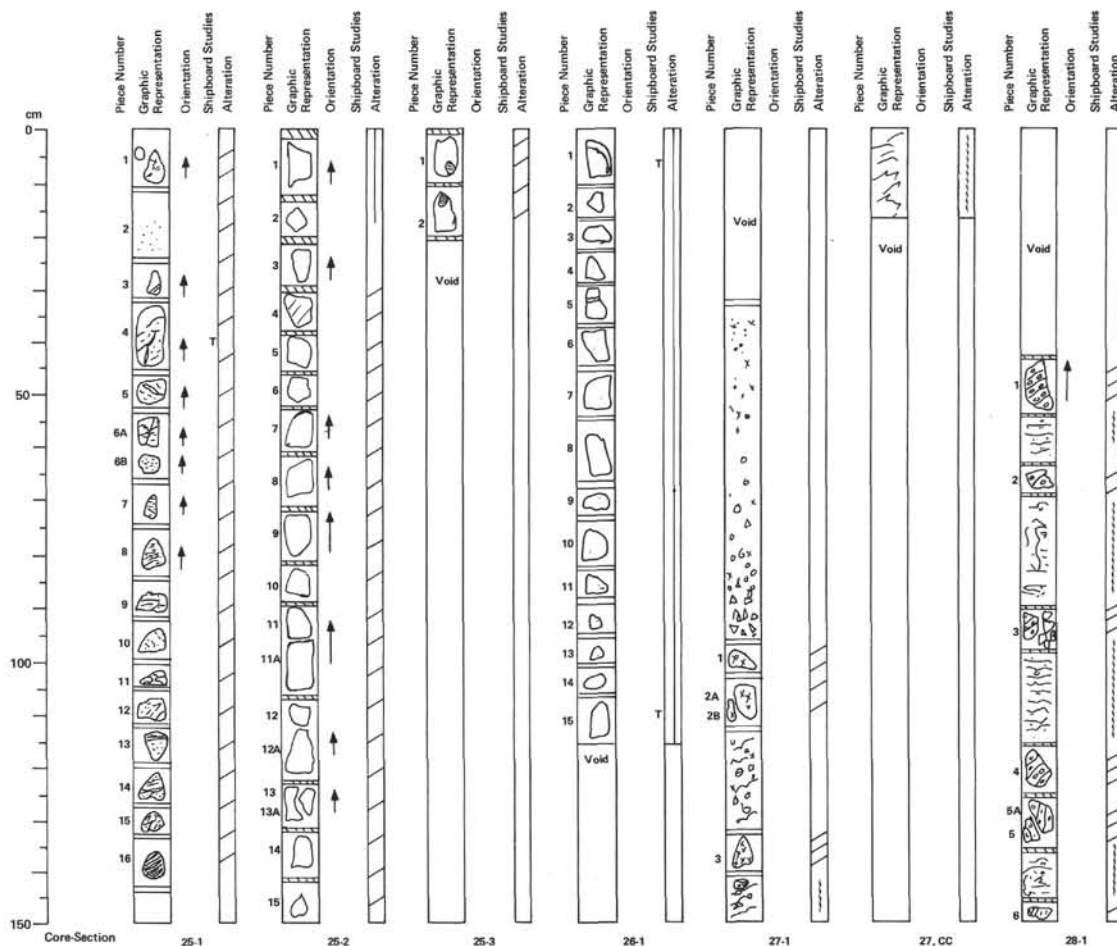
TIME – ROCK UNIT	BIOSTRATIGRAPHIC ZONE	FOSSIL CHARACTER			SECTION METERS	GRAPHIC LITHOLOGY	DRILLING DISTURBANCE STRUCTURES	SAMPLES	LITHOLOGIC DESCRIPTION
		FORAMINIFERS	NANNOFOSSILS	RADIOLARIANS					
					0.5 1 1.0 CC				Dominant lithology: igneous rock. i) Basalt. ii) Gabbro – predominantly.

SITE 567 HOLE A CORE 27 CORED INTERVAL 445.8–455.5 m sub-bottom

TIME – ROCK UNIT	BIOSTRATIGRAPHIC ZONE	FOSSIL CHARACTER			SECTION METERS	GRAPHIC LITHOLOGY	DRILLING DISTURBANCE STRUCTURES	SAMPLES	LITHOLOGIC DESCRIPTION
		FORAMINIFERS	NANNOFOSSILS	RADIOLARIANS					
					0.5 1 1.0 CC				Dominant lithology: igneous rock. i) Meta gabbro. ii) Micro-gabbro.  Drilling breccia.  Serpentine mud

SITE 567 HOLE A CORE 28 CORED INTERVAL 455.5–474.9 m sub-bottom

TIME – ROCK UNIT	BIOSTRATIGRAPHIC ZONE	FOSSIL CHARACTER			SECTION METERS	GRAPHIC LITHOLOGY	DRILLING DISTURBANCE STRUCTURES	SAMPLES	LITHOLOGIC DESCRIPTION
		FORAMINIFERS	NANNOFOSSILS	RADIOLARIANS					
					0.5 1 1.0				Dominant lithology: igneous rock. i) Serpentinized peridotite. ii) Serpentine mud.



## 84-567A-25-1

Piece 1: meta-gabbro of greenschist facies with greenish yellow veins.

Piece 2: gabbro drill breccia.

Pieces 3–16: meta-basalt containing calcite veins and thin reddish brown alteration layers.

## 84-567A-25-2

Depth: 5958.6–5967.5 m

Pieces 1–3: very fine dusky red (5R 3/4) to very dark red (5R 2/6) and very dusky red (10R 2/2) altered meta-basalt(?)

Pieces 4–15: very fine greenish black (5GY 2/1) meta-gabbro/diabase with phenocrysts of olivine and calcite-filled vesicles. This rock is heavily fractured, filled in some places with the red material described above.

## 84-567A-25-3

Depth: 5958.6–5967.5 m

Pieces 1 and 2: as in 567A-25-2, Pieces 4–15,

## 84-567A-26-1

Depth: 444.7–445.8 m

Pieces 1–3: dusky green (5G 3/2) to dusky red (10R 2/2) meta-basalt with chlorite and calcite veins. Shape and alteration along rim of sample 1 suggests it may be the rim of a pillow.

Pieces 4–15: greenish (10G 4/2) greenschist facies meta-gabbro.

## 84-567A-27-1

Depth: 445.8–445.5 m

0–34 cm: void.

34–94 and 113–131 cm: olive black (5Y 2/1) graded drill breccia of meta-gabbro.

96–100, 103–110, and 122–138 cm: 3 pieces of greenschist facies meta-gabbro. Greenish black (5G 2/1) with plagioclase altered to actinolite and clinzoisite, and chlorite ~80%, amphibolite and clinopyroxene <30%, opaque minerals (magnetite and chromite) <10%, and calcite veins <2%.

142–150 cm: medium bluish gray (5B 5/1) serpentinite mud with small pieces of meta-gabbro and serpentinite.

## 84-567A-27-CC

Depth: 5974.8–5984.5 m

0–15 cm: medium bluish gray (5B 5/1) serpentinite mud.

## 84-567A-28-1

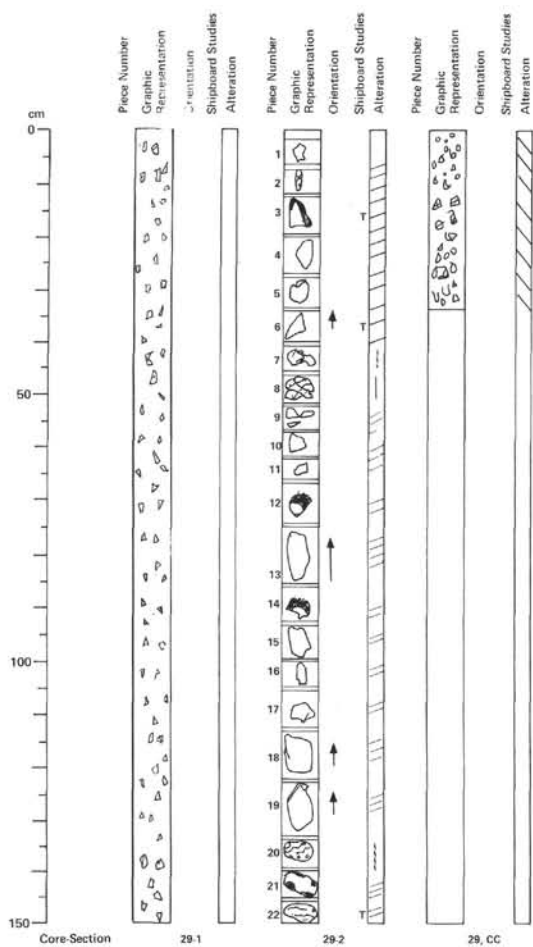
Depth: 8003.9–8013.6 m

0–45 cm: void.

Pieces 1–6 are massive greenish black to black serpentinite.

56–63, 71–88, 97–112, and 137–144 cm: medium blue (5B 5/1) serpentinite mud.

SITE 567		HOLE A		CORE 29		CORED INTERVAL		474.9-494.3 m sub-bottom			
TIME - ROCK UNIT	BIOSTRATIGRAPHIC ZONE	FOSSIL CHARACTER				SECTION	METERS	GRAPHIC LITHOLOGY	GRILLING DISTURBANCE STRUCTURE STRIATIONS	SAMPLES	LITHOLOGIC DESCRIPTION
		FORAMINIFERS	NANNOFOSSILS	RADIOLARIANS	DIATOMS						
										</	



84-567A-29.1

Depth: 498.0–498.5 m

0–150 cm: drill breccia containing pieces of serpentinite, meta-gabbro, meta-diorite, meta-basalt. Larger pieces were separated and oriented where possible and are described in 95-567A-29.2.

84-567A-29.2

499.5–501.0 m

Pieces 1, 3–6, 8–19, and 21: serpentinite (black – N1) and dark green with veins of talc or chrysotile.

Piece 2: gabbro with >50% plagioclase; 30% pyroxene, 10% actinolite/chlorite, 5% opaques (spinel, chromite, magnetite), 3% carbonate veins.

Pieces 7 and 20: dusky blue (SPB 3/2) serpentinite mud with pieces of massive serpentinite.

Piece 22: altered basalt containing serpentinite in vesicles.

84-567A-29. CC

Depth: 494.6–501.0 m

0–34 cm: drill breccia with pieces of serpentinite, gabbro, altered basalt, 0.5–3 cm diameter.



